DOCKET NO. **SA- 516**

EXHIBIT NO. **20R**

NATIONAL TRANSPORTATION SAFETY BOARD
WASHINGTON, D.C

The Laboratory Characterization of Arco Jet Fuel Vapor and Liquid

(79 Pages)

THE LABORATORY CHARACTERIZATION OF ARCO JET FUEL VAPOR AND LIQUID

Final Report

Prepared for the National Transportation Safety Board

by

James E. Woodrow

Faculty Research Associate

Center for Environmental Sciences and Engineering

University of Nevada

Reno, NV 89557-0187

June, 2000

Abstract

Jet fuel -- its liquid and vapor -- was characterized as part of the National Transportation Safety Board's (NTSB's) investigation into the cause of the TWA Flight 800 accident (DCA96MA070; the crash of a 747-131, N93119). For the vapor, headspace gas chromatography was used to measure component partial pressures and total vapor pressures for ten jet fuel samples (Jet-A) provided by the Atlantic Richfield Company (ARCO). These characteristics derived from the fuel vapor were also derived from analysis of the neat liquid for eight of these fuel samples, and the results of the two analytical approaches were compared. Three of the fuel samples were taken from fuel used in the quarter-scale tests #42, 46, and 51 designed to simulate possible fuel tank conditions at the time of the accident. Seven of the ARCO samples had been reformulated to alter the flash point. Two additional samples (giving a total of twelve) were taken from the center wing tank of a 747 aircraft involved in ground tests in Marana, AZ. Measurements of all of the fuel vapor samples were made at 40°C, 50°C, and 60°C and at vapor volume-to-liquid volume (V/L) ratios of 274 (nearly empty tank; ~3 kg/m^3) and 1.2 (half-filled tank; ~400 kg/m^3). Characterization of the liquid fuels was done by simple injections of the neat liquids onto a temperature-programmed gas chromatograph.

Acknowledgments

The author gratefully acknowledges the technical assistance, helpful suggestions, and encouragement of Dr. Merritt Birky and Joseph Kolly, with the National Transportation Safety Board, and professor Joseph Shepherd, California Institute of Technology, Graduate Aeronautical Laboratories. Thanks, also, to Dr. John Sagebiel, Desert Research Institute, for the many helpful discussions of his and my work related to the TWA 800 investigation. This report was submitted in fulfillment of contractual obligations by the Center for Environmental Sciences and Engineering, University of Nevada, Reno, under the sponsorship of the National Transportation Safety Board. Work was completed as of February 29, 2000.

Table of Contents

page

Abstract i

Acknowledgments ii

List of Figures iv

List of Tables v

Introduction 1

Procedures 1

Headspace (vapor) method 2

Liquid fuel method 4

Results and Discussion 6

Headspace (vapor) Method 6

Liquid Fuel Method 17

Half-filled tank (400 kg/m^3 [V/L = 1.2]) 19

Nominal loading (3 kg/m^3 [V/L = 274]) 31

Summary 37

References 39

Appendix A: Headspace GC results for the ARCO fuel samples and the Marana, AZ, ground test fuel samples 41

Appendix B: Vapor data calculated from the liquid GC results for the ARCO fuel samples 60

List of Figures

page

Figure 1. Typical headspace gas chromatogram of Jet-A vapor showing standard retentions (carbon numbers 5-12) and subsections (vertical lines)....5

Figure 2. Typical jet-a liquid chromatogram and n-alkane (C_5-C_{20}) retention times.....7

Figure 3. Comparison of relative vapor density (A) and partial pressure (B) for ARCO, ground test, and Reno fuels. (V/L = 1.2) 10

Figure 4. Comparison of relative vapor density for quarter-scale test #42 fuel at V/L=1.2 and 274 (A) and variation of relative vapor density with temperature for fuel #42 at V/L=274 (B).....12

Figure 5. Comparison of vapor composition (A) and saturation vapor pressure (B) for ARCO fuels at 40°C and V/L=1.2.....16

Figure 6. Instrument response vs. hydrocarbon vapor density.....30

List of Tables

page

Table 1. Liquid jet fuel samples supplied by ARCO, California Institute of Technology (CIT), and Evergreen for fuel vapor characterization 3

Table 2. ARCO test fuels for flash flammability testing.....14

Table 3. Flash point and vapor pressure vs. temperature regression curves for the ARCO jet fuel samples.....15

Table 4. Fuel/air mass ratios and fuel mole fractions for the flash point ARCO jet fuel samples, quarter-scale samples, and ground test samples at nominal loading.....18

Table 5. Subsection mole percent for liquid ARCO fuel samples.....20

Table 6. Calculated total vapor pressure and average molecular weight for liquid ARCO fuel samples.....21

Table 7. Comparison of vapor density and average vapor molecular weight derived from vapor and liquid ARCO jet fuel characterization 24

Table 8. Flash point and vapor pressure vs. temperature regression curves for liquid ARCO jet fuel samples.....25

Table 9. Fuel/air mass ratios (FARs) for the ARCO fuels at their flash points.....26

Table 10. Comparison of ARCO jet fuel vapor pressures derived from vapor and liquid characterization 28

Table 11. Example comparisons of liquid fuel mole fractions derived from vapor and liquid characterization 29

Table 12. Comparison of liquid mole fractions derived from C_5-C_{12} and C_5 only regression equations applied to the vapor characterization of the Base Jet fuel (quarter-scale test #46) 32

Table 13. Measured and calculated vapor pressures for the ARCO jet fuels under nominal loading conditions (V/L = 274 [~3 kg/m^3]) 34

Table 14. Liquid-vapor hydrocarbon distribution coefficients for the ARCO jet fuels ...35

Table 15. Comparison of vapor pressure vs. temperature regressions derived from liquid and vapor characterization for the ARCO jet fuel samples at nominal loading (3 kg/m^3).....36

Table A-1. Headspace GC results for ARCO samples at 40°C (10 mL [V/L = 1.2]) 42

Table A-2. Headspace GC results for ARCO samples at 40°C (0.08 mL [V/L = 274]) 44

Table A-3. Headspace GC results for ARCO samples at 50°C (10 mL [V/L = 1.2]) 46

Table A-4. Headspace GC results for ARCO samples at 50°C (0.08 mL [V/L = 274]) 48

Table A-5. Headspace GC results for ARCO samples at 60°C (10 mL [V/L = 1.2]) 50

Table A-6. Headspace GC results for ARCO samples at 60°C (0.08 mL [V/L = 274]) 52

Table A-7. Headspace GC results for the ground test fuel samples at 40°C (10 mL [V/L = 1.2]).....54

Table A-8. Headspace GC results for the ground test fuel samples at 40°C (0.08 mL [V/L = 274]).....55

Table A-9. Headspace GC results for the ground test fuel samples at 50°C (10 mL [V/L = 1.2]).....56

Table A-10. Headspace GC results for the ground test fuel samples at 50°C (0.08 mL [V/L = 274]).....57

Table A-11. Headspace GC results for the ground test fuel samples at 60°C (10 mL [V/L = 1.2]).....58

Table A-12. Headspace GC results for the ground test fuel samples

at 60°C (0.08 mL [V/L = 274])..... 59

Table B-1. Liquid GC results for ARCO samples at 40°C (10 mL [V/L = 1.2])..... 61

Table B-2. Liquid GC results for ARCO samples at 40°C (0.08 mL [V/L = 274])..... 63

Table B-3. Liquid GC results for ARCO samples at 50°C (10 mL [V/L = 1.2])..... 65

Table B-4. Liquid GC results for ARCO samples at 50°C (0.08 mL [V/L = 274])..... 67

Table B-5. Liquid GC results for ARCO samples at 60°C (10 mL [V/L = 1.2])..... 69

Table B-6. Liquid GC results for ARCO samples at 60°C (0.08 mL [V/L = 274])..... 71

Table B-7. Fuel/air mass ratios and fuel mole fractions at nominal loading (V/L = 274 [~3kg/m^3]) derived from the liquid characterization of the eight ARCO jet fuel samples..... 73

Introduction

As part of the National Transportation Safety Board's (NTSB's) investigation into the cause of the TWA Flight 800 accident (DCA96MA070; crash of a 747-131, N93119), the characteristics of jet fuel (Jet-A) -- its liquid and vapor -- were determined. For the fuel vapor, a headspace gas chromatographic (HS-GC) method, described in detail in earlier reports (Woodrow and Seiber, 1988 and 1989), was used to determine component partial pressures and total vapor pressures of a dozen samples of jet fuel (Woodrow and Seiber, 1997), some of which represented the type of fuel used in commercial aviation and some of which were fuel samples reformulated to vary the flash point. Using this method, it was possible to accurately determine vapor pressures by modeling the jet fuel vapor, characterized by a complex mixture of hydrocarbons, with just a few n-alkane reference standards. This approach (i.e., modeling the fuel with a few n-alkane reference standards) was used to determine component partial pressures and total vapor pressures of eight of the liquid fuels for comparison with the vapor results. An important goal of this study was to provide technical information about the properties of jet fuel and its vapor under conditions that might have existed in the Flight 800 center wing fuel tank at the time of the accident. Specifically, we wanted to address the question of fuel flammability under flight conditions at 14,000 feet. It is hoped that this information will contribute to a better understanding of the nature of the accident and to the formulation and design of safer fuels and fuel tanks. This report, summarizing our 1998 and 2000 work, is an outgrowth of an earlier NTSB-sponsored study of commercial jet fuel characteristics, completed in 1997 and summarized in a report submitted to the NTSB in November of that year (Woodrow and Seiber, 1997).

Procedures

In September, 1998, the California Institute of Technology (CalTech), Graduate Aeronautics Laboratory, shipped to the University of Nevada (UNR) seven liquid jet fuel samples formulated by the Atlantic Richfield Company (ARCO) to have a range of flash points. In June, 1998, Evergreen Air Center, on behalf of Boeing, shipped two liquid jet

fuel samples taken from the center wing tank (CWT) of a 747 aircraft that had been part of ground tests in Marana, AZ. Finally, three additional liquid jet fuel samples taken from quarter-scale tests #42, 46, and 51 were shipped to UNR by CalTech personnel. These latter samples were taken from the ARCO base jet fuel supply, and they were used in the quarter-scale tests to determine if there were any systematic changes in the fuel stock over the course of the test series. Sample designations and descriptions are summarized in Table 1. All samples were stored in a laboratory refrigerator at 1-2°C.

The two ground test samples were taken from tests #1 and #3. For test #1, the CWT contained approximately 50 gallons of Jet-A and there was no environmental control system (ECS) insulation. Test #3 was essentially a repeat of test #1, except that the CWT contained approximately 1800 gallons of Jet-A. During test #1, steel canisters were provided by Desert Research Institute (DRI) personnel (Dr. John Sagebiel) to sample the CWT ullage at 1, 2, and 3 hours into the test, and after 3 hours for test #3 (Sagebiel, 1998).

Headspace (vapor) method. Into separate chilled 22 mL glass headspace vials (Perkin-Elmer, Norwalk, CT) were placed 0.08 mL and 10 mL of chilled liquid fuel samples, and the vials were immediately sealed with Teflon®-lined septa in crimped aluminum caps. These volumes of fuel represented vapor volume-to-liquid volume (V/L) ratios of 274 and 1.2, respectively (i.e., an almost empty fuel tank and an approximately half-filled tank). The sealed samples were placed in an HS-40 autosampler and injector (Perkin-Elmer), where they were thermostated at 40°C, 50°C, and 60°C for at least 30 min. After the samples were thermostated, the HS-40 automatically punctured the septa with a hollow sampling needle, the vials were pressurized to about 150 kPa, the equilibrated vapor was sampled for 0.01 min, the resulting vapor aliquot was injected onto a 60 m x 0.32 mm (i.d.) DB-1 fused silica open tubular (FSOT) capillary column (J&W Scientific, Folsom, CA), and the chromatographed vapor was detected by a flame ionization detector. The column was held at 100°C for 4 min, after which time it was programmed at 2°/min to

Table 1. Liquid jet fuel samples supplied by ARCO, California Institute of Technology (CIT), and Evergreen for fuel vapor characterization.

Sample Designation	Sample Description
Base Jet[a]	ARCO; LIMS# 80036458
2.5%OH	ARCO; Base Jet + 9% of 2.5W% OH; LIMS# 80049765
97.5%	ARCO; 97.5 wt% Btm; LIMS# 80036460
95%	ARCO; 95.0 wt% Btm; LIMS# 80036732
92.5%	ARCO; 92.5 wt% Btm; LIMS# 80037890
90%	ARCO; 90.0 wt% Btm; LIMS# 80039332
87.5%	ARCO; 87.5 wt% Btm; LIMS# 80039902
85%	ARCO; 85.0 wt% Btm; LIMS# 80039903
#42	CIT (ARCO); quarter-scale test #42
#46	CIT (ARCO); quarter-scale test #46
#51	CIT (ARCO); quarter-scale test #51
#1	Evergreen; ground test #1; 50 gal fuel in CWT[b]; no ECS[c] insulation
#3	Evergreen; ground test #3; 1800 gal fuel in CWT; no ECS insulation

[a] Same as quarter-scale fuel sample #42.

[b] CWT = center wing tank.

[c] ECS = environmental control system.

140°C, where it was held for 1 min. The column carrier gas (helium) flow rate was about 3 mL/min, which means that for an injection time of 0.01 min, the volume of vapor sample injected was about 30 μL (i.e., 3 mL/min x 0.01 min x 1000 μL/mL).

The fuel samples were evaluated using a mixed hydrocarbon standard, which consisted of an equal volume mix of the normal alkanes pentane (C_5) through dodecane (C_{12}) (tridecane [C_{13}] at 60°C). Into separate chilled headspace vials were placed 1, 0.5, 0.25, and 0.1 μL of the mixed standard and the sealed vials were processed in the same way as for the fuel samples. These volumes of mixed standard were low enough to allow the hydrocarbons to completely vaporize, so that eight separate vapor density standard curves (nine at 60°C) could be generated for each volume of mixed standard. Using the gas chromatographic retention times of the hydrocarbon standards, the fuel vapor chromatograms were divided into eight or nine subsections, each of which was approximately centered about the retention time of a hydrocarbon standard (Figure 1). The peak areas in each subsection were summed and treated as a single peak in the vapor density regression equations to calculate subsection vapor densities, which were used to calculate subsection partial pressures. All of the subsection partial pressures were summed to obtain total vapor pressures for the fuel samples.

Liquid fuel method. The goal using this method was to characterize eight samples of the liquid ARCO fuels (Base Jet [quarter-scale test #46] and the seven reformulated fuels) using the techniques that were applied to the characterization of the fuel vapor. To reach this goal, the liquid composition of each fuel was modeled using sixteen alkane reference standards (C_5-C_{20}), with the results expressed as mole percent for each of the sixteen subsections, partial pressure for each subsection, and the overall vapor pressure of each fuel.

Each of the eight fuel samples was injected as the neat liquid (0.1-0.2 μL) onto a 60 m x 0.32 mm (i.d.) DB-1 FSOT capillary column (J&W Scientific) and each hydrocarbon component was monitored using a flame ionization detector installed in a Hewlett-Packard

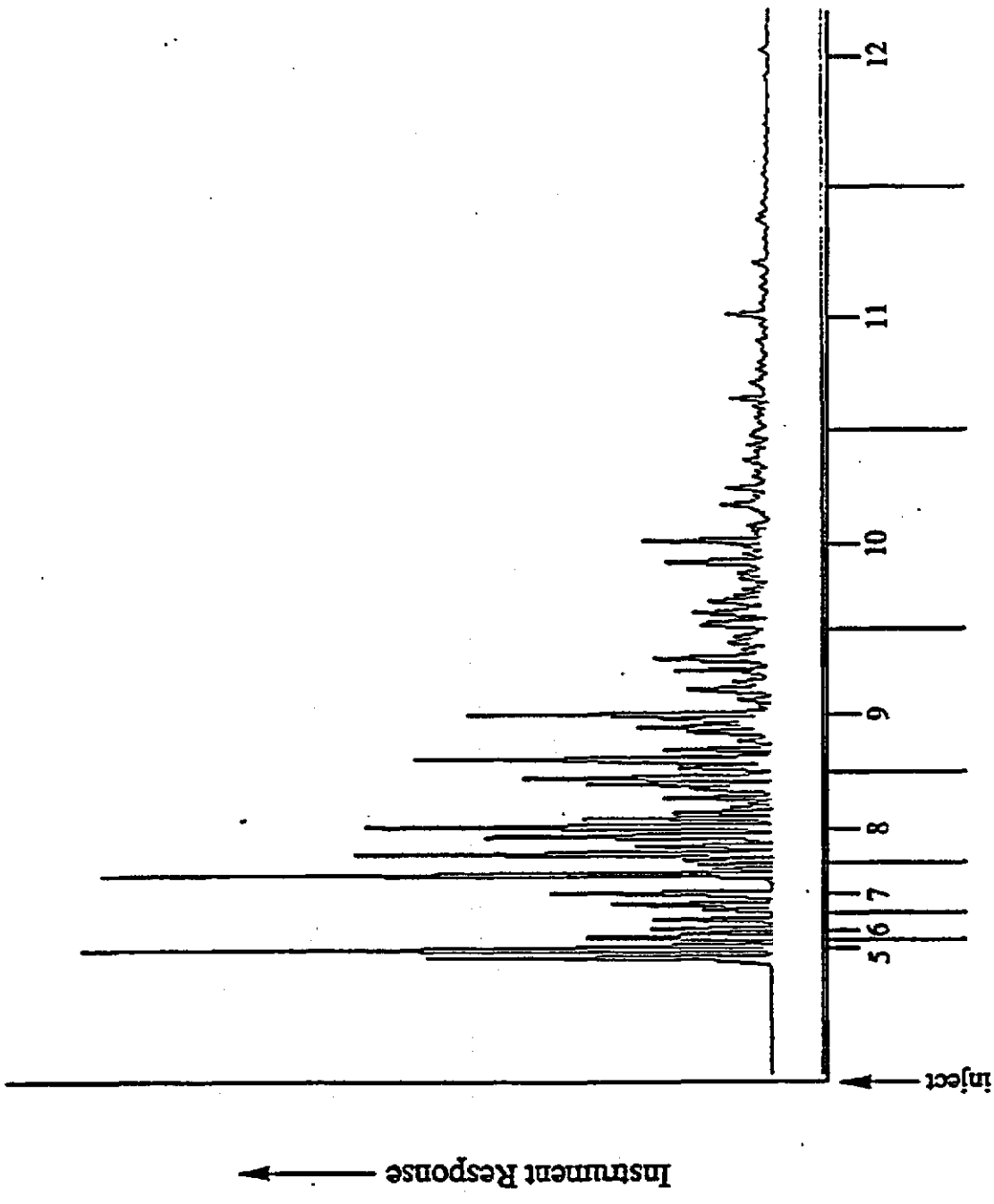

Figure 1. Typical headspace gas chromatogram of Jet-A vapor showing standard retentions (carbon numbers 5-12) and subsections (vertical lines).

model 5890 Series II gas chromatograph. All samples were automatically injected using a computer-controlled enhanced autoinjector with a nanoliter adapter installed (Agilent, San Fernando, CA). The capillary column was held at 50°C for four minutes, programmed at a rate of 1°C/min to 250°C, where it was held for ten minutes. Each run took about 3.6 hours to complete. Starting with eicosane (C_{20}), and working down in carbon number, a mixed hydrocarbon standard (pentane through eicosane) was prepared by weighing each component as it was added to the mixture. The mixed standard was chromatographed under the same conditions used for the liquid fuel samples. Based on elution times for the reference hydrocarbons, each fuel chromatogram was divided into sixteen subsections, with each subsection centered approximately on its respective reference hydrocarbon (Figure 2). By injecting different amounts of the standard mixture, regression equations (GC peak area vs. mass of hydrocarbon injected) were generated for each fuel subsection. From these regression equations, a mass for each of the sixteen subsections was derived using the summed peak area for each subsection. Each subsection mass was then divided by the molecular weight of the reference hydrocarbon, giving the number of moles for each subsection, from which subsection mole fraction was derived. Using Raoult's law, with the subsection mole fractions and saturation vapor pressures for the reference hydrocarbons, subsection partial pressures could be calculated at any given temperature.

Results and Discussion

Headspace (vapor) Method

Analysis using headspace sampling and gas chromatography (GC) requires thermodynamic equilibrium between a condensed phase and its vapor phase in a sealed container so that aliquots of the vapor can be removed for quantitative GC analysis. For a liquid fuel mixture in equilibrium with its vapor in a sealed container, GC response of a component in the vapor is proportional to the vapor density. This means that measuring the GC response essentially measures the partial pressure if the instrument calibration factor is known. The calibration factor has a specific value for each component in the fuel mixture

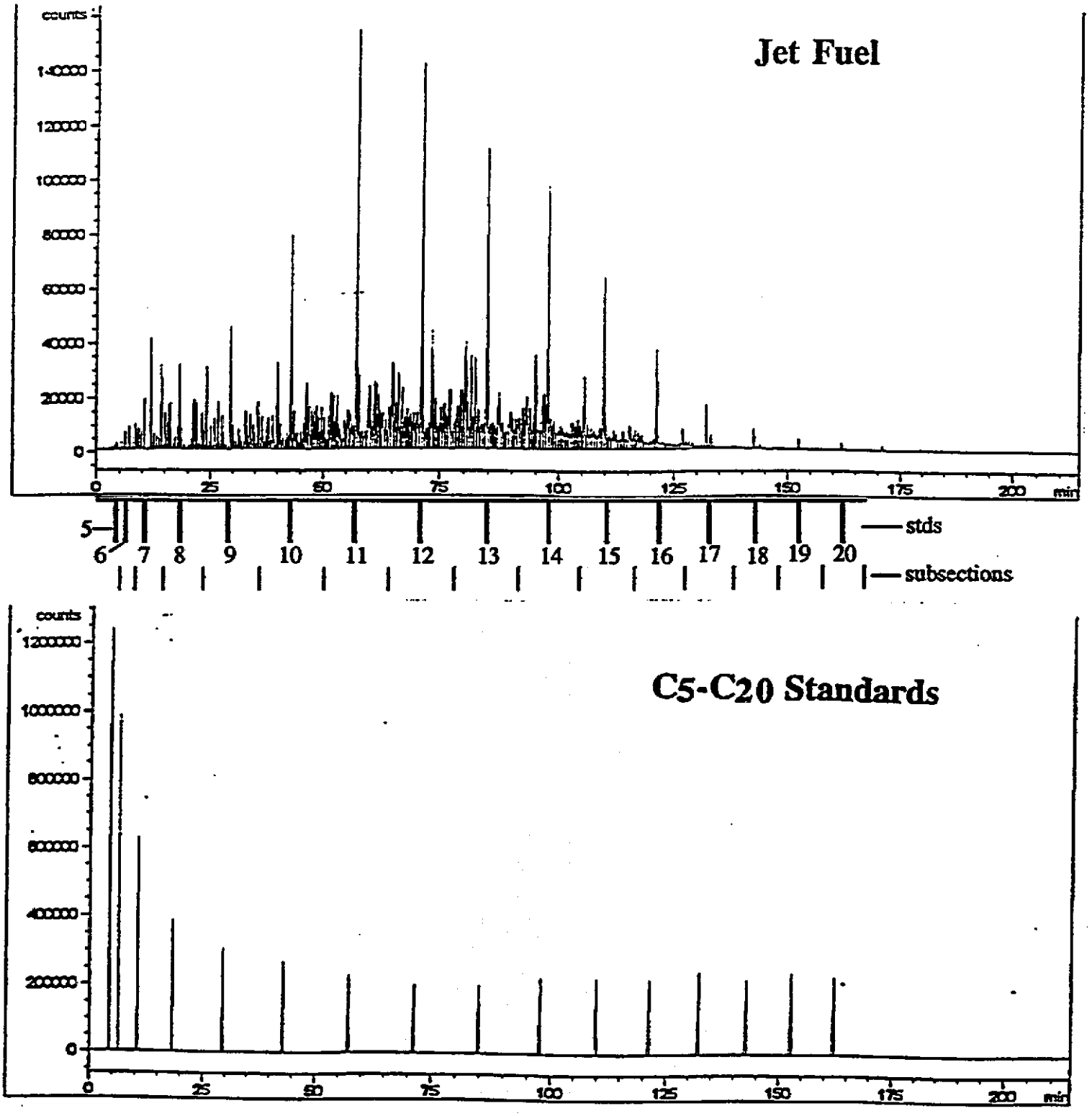

Figure 2. Typical jet-a liquid chromatogram and n-alkane (C5-C20) retention times.

and depends on the characteristics of the detector used. However, the complex jet fuel mixture can be represented by a relatively small number of n-alkane reference standards and the properties of the standards can be attributed to the fuel mixture. In other words, a single n-alkane reference standard can be used to represent a summation of GC responses (subsection of the fuel GC) for a series of components in the jet fuel vapor. Each subsection n-alkane reference standard is used to generate a standard curve, which is a correlation of instrument response with vapor mass density (g/L). Then, the partial pressure (P_i) corresponding to each subsection is obtained from the ideal gas law and the molecular weight of the n-alkane reference standard for each subsection. That is,

$$P_i = (n/V)_i \cdot R \cdot T \cdot 1013.232 \qquad (1)$$

where i = 5,...,12, $(n/V)_i$ is the vapor molar density (mole/L), R is the gas constant (0.08205 L-atm/°K•mole), T is absolute temperature, and 1013.232 is a factor to convert atmospheres to mbars. Also, $(n/V)_i = (g/L)/(mw)_i$, where (g/L) is the vapor mass density obtained from the subsection standard curve and $(mw)_i$ is the molecular weight of the subsection reference hydrocarbon. The total vapor pressure (P_{5-12}) for the fuel sample is, then, just simply a summation of the individual partial pressures:

$$P_{5-12} = \Sigma P_i \qquad (2)$$

No correction for real gas behavior is necessary since component partial pressures remain far below the critical pressures.

An important objective of this study was to use the described vapor method to determine component partial pressures and total vapor pressures of samples of jet fuel representative of the type of fuel used in commercial aviation and of a series of fuel samples which had been reformulated to vary the flash point. The analytical instrumentation sampled the sealed vials using a pneumatic-balanced pressure principle which avoids the disadvantages associated with gas syringes, such as change of partial pressures of the volatiles due to reduced pressure in the syringe (Ioffe and Vitenberg, 1984a). In a typical operation utilizing the pneumatic-balanced pressure principle, the septum of the

thermostated sample was pierced by the hollow sampling needle, the vial was pressurized to either equal or exceed the head pressure of the FSOT column, gas flow to the FSOT column was temporarily interrupted, causing the column head pressure to decrease, and then an aliquot of the headspace was injected onto the FSOT column using the vial pressure as the driving force.

The volumes of the mixed hydrocarbon standard were low enough to assure complete vaporization of the C_5-C_{13} hydrocarbons under the test conditions. For the higher molecular weight hydrocarbons (e.g., dodecane and tridecane), 0.5 μL and less of the hydrocarbon mix was used to assure complete vaporization. The resulting vapor densities (g/L) for the reference hydrocarbons were correlated with their gas chromatographic peak areas to generate eight individual calibration curves (nine at 60°C) that were used to calculate subsection partial pressure. These eight or nine regression equations were linear, with correlation coefficient (r^2) values close to unity. Each subsection summed GC peak area (5-13) was treated as an individual compound and was used in the appropriate subsection regression equation to calculate a vapor density. As described above, the molecular weights of the subsection reference hydrocarbons were then used to convert the mass densities to molar densities for use in the ideal gas equation (equation 1).

Results for the ten ARCO fuel samples and the two Marana ground test samples are summarized in Appendix A as Tables A-1 through A-12. These tables include subsection and total vapor pressure (mbar), subsection mole percent, and subsection vapor density (g/m^3) for the fuel samples at 40°C, 50°C, and 60°C and for two V/L ratios (i.e., 274 and 1.2). Based on the mole percent values, average molecular weights of the fuel vapor were computed for each V/L ratio at each temperature.

Figure 3 compares the ARCO fuels taken from the quarter-scale tests #42, 46, and 51 (designated Base Jet [ARCO]), the fuel used in the ground tests in Marana, AZ (samples #1 and #3), and a sample of fuel obtained locally from the Reno/Tahoe International Airport (Reno – supplied by Exxon). The Reno and ground test fuels had vapor compositions

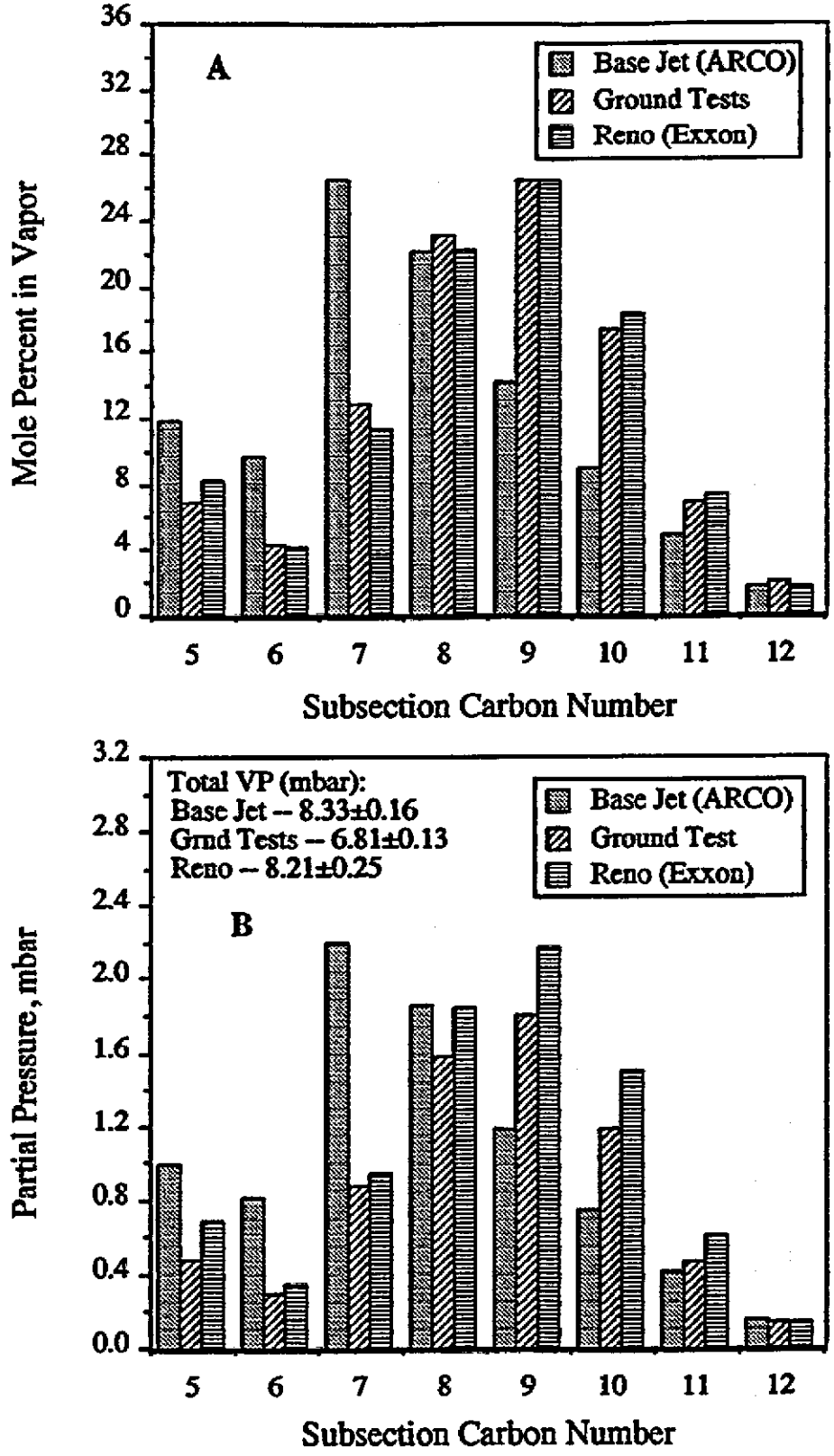

Figure 3. Comparison of relative vapor density (A) and partial pressure (B) for ARCO, ground test, and Reno fuels at 40°C. (V/L = 1.2).

with hydrocarbon distributions centering approximately about subsection carbon number 9, whereas the hydrocarbon distribution for the ARCO Base Jet fuel vapor centered approximately about carbon number 7 (Figure 3A). This relative vapor composition is also reflected in the average molecular weights for the fuel vapors – about 121 for the Reno and ground test fuels compared to about 110 for the ARCO fuel. However, the ARCO and Reno (Exxon) fuels had similar saturation vapor pressures, while the average vapor pressure for the ground test fuels was about 15-20% less, indicating some possible weathering of these fuels (Figure 3B). The ARCO fuel was shipped in a sealed drum directly from the formulator via CalTech personnel and the Reno fuel was obtained directly from the sump of a refueling truck, but the ground test fuel samples were taken from the center wing tank of a Boeing 747 aircraft after fueling under the relatively hot conditions of late Spring in Arizona.

As reported earlier (Woodrow and Seiber, 1997), a decline in relative vapor density (mole percent) was substantial for subsection carbon number 5 in going from an approximately half-filled tank (V/L = 1.2) to a nearly empty tank (V/L = 274), whereas for higher carbon numbers, changes in relative vapor density were minor. For example, the ARCO sample from quarter-scale test #42 showed a decline in subsection 5 by a factor of 6-8, whereas subsection carbon number 7, for example, showed a slight decline by a factor of 1-1.2, as illustrated in Figure 4A. A similar behavior was exhibited by the specially formulated ARCO samples, except that in some cases changes in relative vapor density for subsection carbon number 5 were even greater (e.g., a factor of 7-15 for ARCO sample 90 wt% Btm). This behavior was reflected in the higher average molecular weights for the nominal loading case compared to the half-filled tank (Tables A-1 through A-12).

However, a 20°C increase in fuel temperature (40°C to 60°C) decreased the relative vapor density for subsection carbon numbers 5 and 7 by only a factor of about 2 and 1.1, respectively, as illustrated in Figure 4B for ARCO sample #42. The conclusion from all of this is that a change in liquid fuel volume by a factor of 125 has a greater effect on vapor

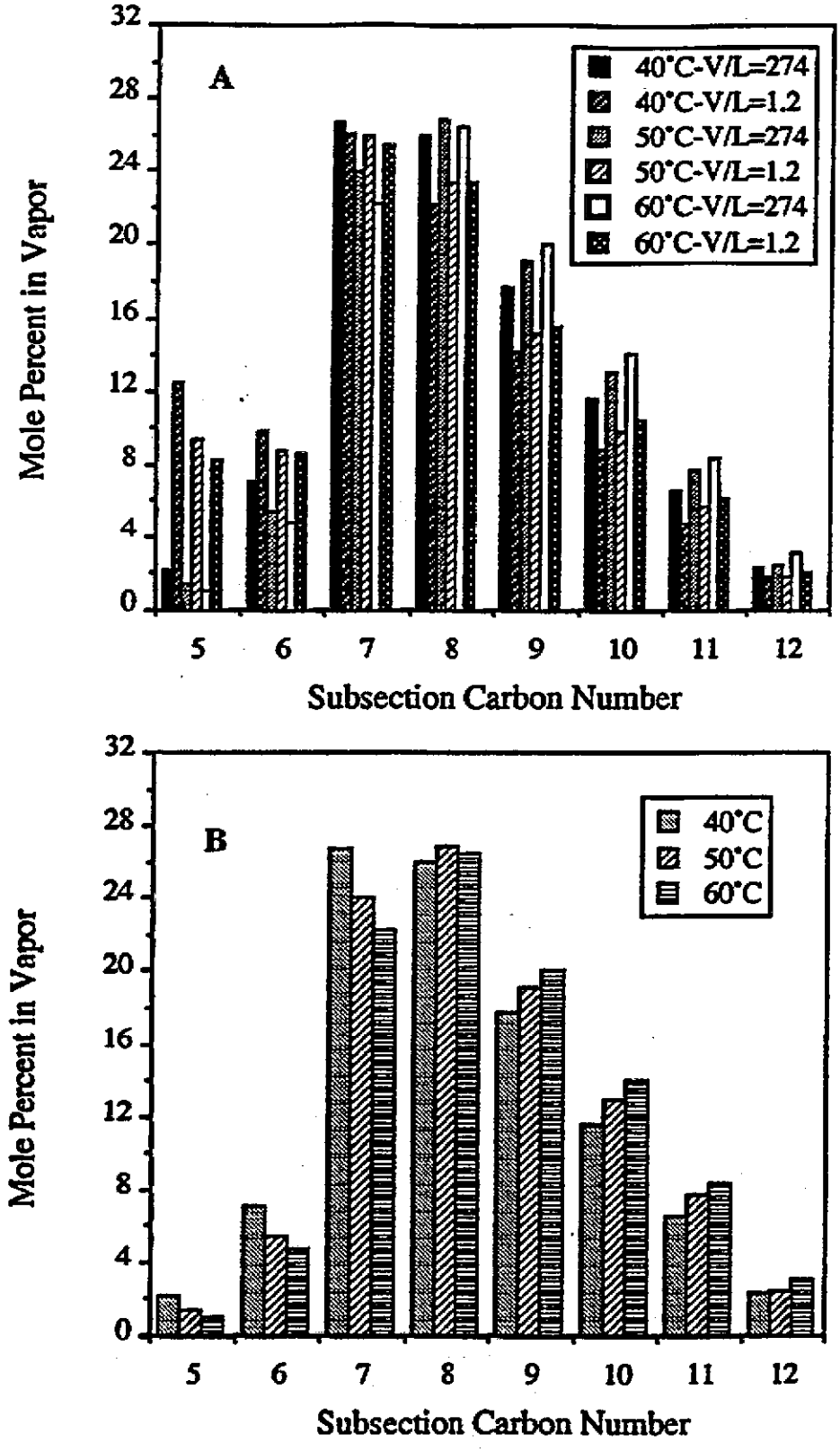

Figure 4. Comparison of relative vapor density for quarter-scale test #42 fuel at V/L=1.2 and 274 (A) and variation of relative vapor density with temperature for fuel #42 at V/L=274 (B).

composition than does a 20° change in temperature.

Table 2 summarizes the properties of the seven ARCO fuel samples formulated to vary the flash point, and, in Table 3, these various fuel flash points are listed along with the fuel vapor pressure vs. temperature regression equations for both the half-filled (~400 kg/m^3) and nominal loading (~3 kg/m^3) cases. With these regression equations and the fuel flash points it is possible to calculate fuel vapor pressure at the flash point and, ultimately, fuel/air mass ratio at the flash point (Shepherd et al., 2000).

The flash point samples listed in Table 2 were created by distillation of the Base Jet fuel using a distillation column and procedure similar to that described in ASTM D2892. First, the Base Jet fuel was distilled and the first 2.5 weight percent of this "overhead" (OH) was collected. The lower flash point (87F) fuel was then created by mixing 91 wt% of the Base Jet and 9 wt% of the OH. The mixture is the fuel designated as 2.5 wt% OH in Table 2. The higher flash point fuels were created by distilling the Base Jet fuel and retaining only a fraction of the "bottom" (Btm) of the distillation. These fuels are designated according to the fraction of the initial fuel weight (by percent) that is used to create the fuel sample. A value of "χ wt% Btm" in the designation means that the initial (100 - χ) wt% that came out of the distillation process was not used. All of this results in one sample of Base Jet, one sample of Base Jet enriched with 9 wt% of light hydrocarbons (2.5 wt% OH), and six samples of concentrated heavy hydrocarbons from the mixture Base Jet, ranging from the lightest in molecular weight (97.5 wt% Btm) to the heaviest (85 wt% Btm).

These prepared samples, with flash points from 87F to 165F, should be compared to the Base Jet sample (quarter-scale tests #42, 46, and 51) which represents the commercial grade jet fuel, with a flash point of 114F. The flash points can be directly related to the composition of the fuel vapor, as illustrated in Figure 5. In this figure, the two flash point extremes (87F and 165F) are compared with the Base Jet fuel. Fuel sample 2.5 wt% OH (flash point = 87F) had a hydrocarbon distribution in the vapor that centered about C_7, whereas hydrocarbon distribution for fuel sample 85 wt% Btm (flash point = 165F)

Table 2. ARCO test fuels for flash flammability testing (Source: ARCO).

Sample	Flash Point (°F)	Distillation (°F)	Acidity (mg KOH/g)	Freeze Point (°F)	Heat of Combustion (BTU/lb)	FIA-Aromatic (Vol%)	Naphthalenes (Vol%)
2.5 wt% OH	87	555	--	ND[a]	--	24.1	2.67
Base Jet[b]	114	556	<0.01	ND	18471	24.4	2.93
97.5 wt% Btm	132	559	0.03	ND	18482	22.4	3
95 wt% Btm	139	559	0.08	ND	18325	23.8	2.9
92.5 wt% Btm	148	561	0.01	<-65	18478	22.5	3.2
90 wt% Btm	159	558	0.034	-43.6	18477	22.5	3.22
87.5 wt% Btm	160	562	0.03	-38.2	18517	22.9	3.31
85 wt% Btm	165	565	0.03	-36.4	18532	22.9	3.42

[a] ND = no data.

[b] The commercial ARCO fuel from which samples were taken for quarter-scale tests #42, 46, and 51 (Tables A-1 through A-6).

Table 3. Flash point and vapor pressure vs. temperature regression curves for the ARCO jet fuel samples.

		Vapor Pressure vs. Temperature Regressions[a]	
Sample	Flash Point, °F (°C)	Vapor Saturation (400 kg/m^3)[b]	Nominal Loading (3 kg/m^3)[c]
2.5 wt% OH	87 (30.6)	Ln VP = 15.294 - 3834.3 (1/T)	Ln VP = 15.303 - 3991.3 (1/T)
Base Jet[d]	114 (45.6)	Ln VP = 15.790 - 4275.3 (1/T)	Ln VP = 14.680 - 4053.3 (1/T)
97.5 wt% Btm	132 (55.6)	Ln VP = 16.505 - 4701.2 (1/T)	Ln VP = 17.716 - 5195.1 (1/T)
95 wt% Btm	139 (59.4)	Ln VP = 16.429 - 4820.7 (1/T)	Ln VP = 18.031 - 5406.3 (1/T)
92.5 wt% Btm	148 (64.4)	Ln VP = 17.022 - 5101.7 (1/T)	Ln VP = 18.856 - 5754.7 (1/T)
90 wt% Btm	159 (70.6)	Ln VP = 17.738 - 5358.1 (1/T)	Ln VP = 19.118 - 5892.9 (1/T)
87.5 wt% Btm	160 (71.1)	Ln VP = 17.149 - 5261.4 (1/T)	Ln VP = 18.109 - 5648.5 (1/T)
85 wt% Btm	165 (73.9)	Ln VP = 16.169 - 5017.6 (1/T)	Ln VP = 18.839 - 5928.7 (1/T)

[a] VP = vapor pressure in mbar; T = °K.

[b] Derived from V/L = 1.2 (Tables A-1, A-3, and A-5).

[c] Derived from V/L = 274 (Tables A-2, A-4, and A-6).

[d] Averaged data for fuel samples from quarter-scale tests #42, 46, and 51 (Tables A-1 through A-6).

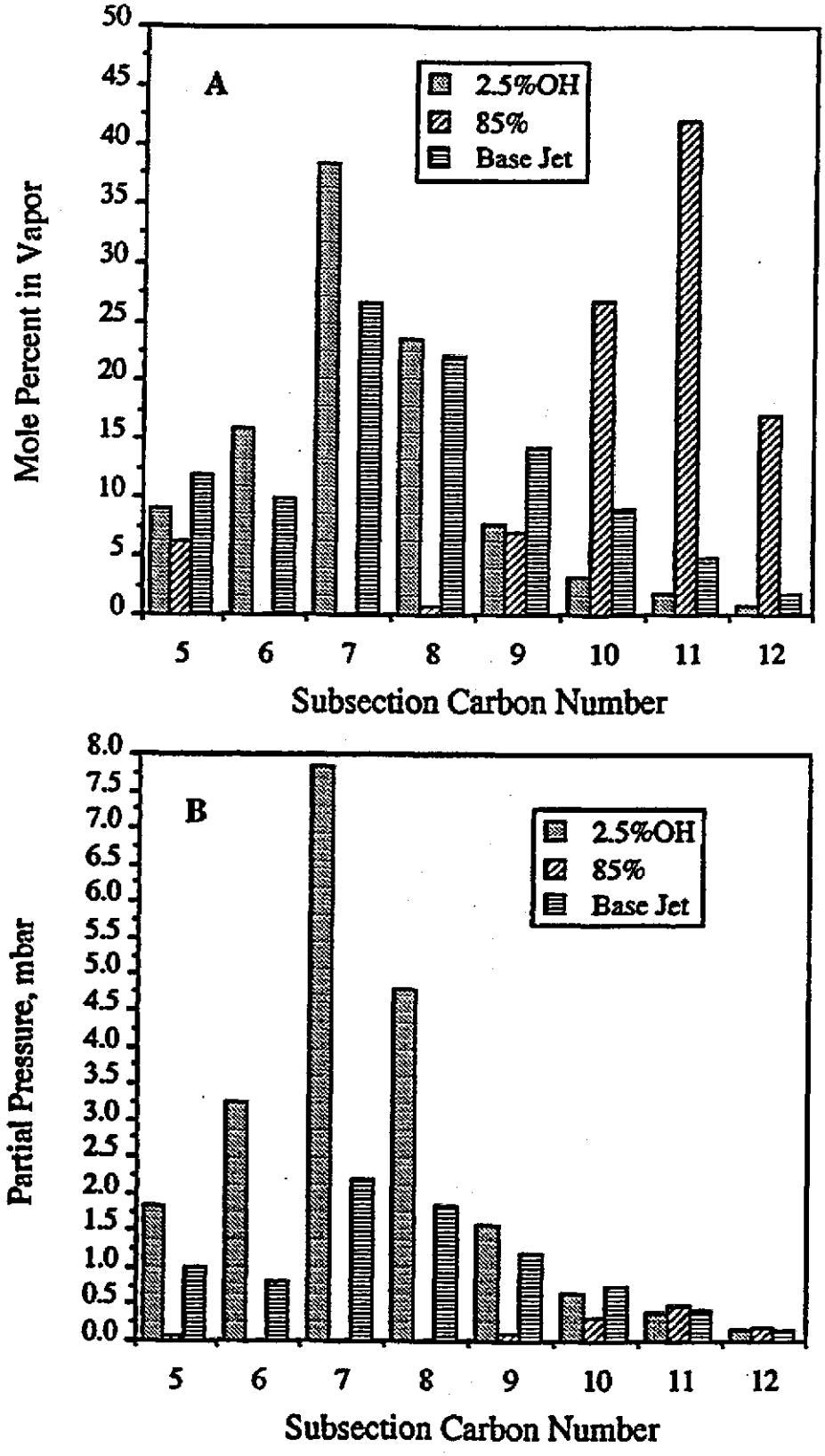

Figure 5. Comparison of vapor composition (A) and saturation vapor pressure (B) for ARCO fuels at 40°C and V/L=1.2.

centered about C_{11} (Figure 5A). In other words, fuels enriched in the heavier, less volatile hydrocarbons had the higher flash points. Furthermore, while sample 85 wt% Btm had detectable hydrocarbons for subsection carbon numbers 5 and 8-12, this sample did not have any detectable hydrocarbons for subsection carbon numbers 6 and 7, except at 60°C where there was some measurable hydrocarbon for subsection 6. It appeared that, based on the subsection pressure and mole percent profiles (Figure 5), sample 85 wt% Btm contained a light hydrocarbon spike.

Table 4 summarizes the calculated fuel/air mass ratios and fuel mole fractions in air at sea level and at 14,000 feet for the nominal fuel loading (V/L = 274; ~3 kg/m^3) at 40°C, 50°C, and 60°C. We used the vapor pressure, molecular weight, and mass density data for the fuel samples (Tables A-2, A-4, A-6, A-8, A-10, and A-12) to make these calculations. Inspection of the data indicates that, compared with a lower flammability limit of about 0.038 fuel/air mass ratio or 0.009 mole fraction (Shepherd et al., 2000), all of the unweathered commercial grade fuels (#42, #46, #51, #1, #3) either equaled or exceeded these values at 40°C and were well within the flammability range at 50°C for the 14,000 foot altitude. However, the flash point ARCO fuel sample 2.5 wt% OH exceeded the limit at sea level and 40°C, whereas the other samples in this group consistently exceeded the limit only at 60°C for 14,000 feet, with the exceptions of sample 90 wt% Btm, which was about equal to the limit, and samples 87.5 wt% Btm and 85 wt% Btm, which were less than the limit.

Liquid Fuel Method

As discussed under **Procedures**, the ARCO liquid fuel chromatograms were divided into sixteen subsections, each of which was represented by a normal alkane reference (Figure 2). However, for direct comparison with the headspace vapor characterization results, much of the liquid characterization results discussed below represent subsections C_5-C_{12} (plus C_{13} at 60°C) only. Appendix B (Tables B-1 through B-7) is a summary of ARCO fuel vapor data derived from the liquid results for subsections C_5-C_{12} (plus C_{13} at

Table 4. Fuel/air mass ratios and fuel mole fractions for the flash point ARCO jet fuel samples, quarter-scale test samples, and ground test samples at nominal loading.

	Fuel/Air Mass Ratio (V/L = 274)					
	40°C		50°C		60°C	
Sample	0 ft[a]	14 kft[b]	0 ft[a]	14 kft[b]	0 ft[a]	14 kft[b]
2.5% OH	0.047	0.081	0.073	0.126	0.104	0.180
97.5%	0.013	0.022	0.022	0.038	0.038	0.066
95%	0.010	0.017	0.016	0.028	0.030	0.052
92.5%	0.008	0.014	0.013	0.022	0.025	0.043
90%	0.007	0.012	0.011	0.019	0.022	0.038
87.5%	0.006	0.010	0.009	0.016	0.017	0.029
85%	0.005	0.009	0.008	0.014	0.016	0.028
#42[c]	0.023	0.040	0.035	0.060	0.051	0.088
#46[c]	0.023	0.040	0.035	0.060	0.050	0.086
#51[c]	0.022	0.038	0.034	0.059	0.050	0.086
#1[d]	0.022	0.038	0.036	0.062	0.055	0.095
#3[d]	0.022	0.038	0.036	0.062	0.057	0.099

	Fuel Mole Fraction (V/L = 274)					
	40°C		50°C		60°C	
Sample	0 ft[e]	14 kft[f]	0 ft[e]	14 kft[f]	0 ft[e]	14 kft[f]
2.5% OH	0.012	0.021	0.019	0.033	0.027	0.047
97.5%	0.003	0.005	0.005	0.009	0.008	0.014
95%	0.002	0.003	0.003	0.005	0.006	0.010
92.5%	0.002	0.003	0.002	0.003	0.005	0.009
90%	0.001	0.002	0.002	0.003	0.004	0.007
87.5%	0.001	0.002	0.002	0.003	0.003	0.005
85%	0.0009	0.002	0.001	0.002	0.003	0.005
#42[c]	0.006	0.010	0.008	0.014	0.012	0.021
#46[c]	0.006	0.010	0.008	0.014	0.012	0.021
#51[c]	0.005	0.009	0.008	0.014	0.012	0.021
#1[d]	0.005	0.009	0.008	0.014	0.012	0.021
#3[d]	0.005	0.009	0.008	0.014	0.013	0.022

[a] Atmospheric mass density (dry air): 1127.4 g/m^3, 40°C; 1092.4 g/m^3, 50°C; 1059.6 g/m^3, 60°C.

[b] Mass ratios at 14 kft were determined by dividing the ratios at sea level by the factor 0.578.

[c] Quarter-scale tests.

[d] Ground tests (Marana, AZ).

[e] Air molar density: 39.1 moles/m^3, 40°C; 37.9 moles/m^3, 50°C; 36.7 moles/m^3, 60°C. Molar densities were determined from the average molecular weight of air (~28.84 g/mole) and the mass densities of air at the various temperatures.

[f] Fuel mole fractions at 14 kft were determined by dividing the fractions at sea level by the factor 0.578.

60°C). Tables B-1 through B-6 include subsection and total vapor pressure (mbar), subsection mole percent, and subsection vapor density (g/m^3) for fuel vapor at 40°C, 50°C, and 60°C and for two V/L ratios (i.e., 274 [3 kg/m^3] and 1.2 [400 kg/m^3]). Based on the calculated mole percent values, average molecular weights of the fuel vapor were computed for each V/L ratio at each temperature. The data in these tables can be compared directly with the headspace vapor data in Appendix A (Tables A-1 through A-6). Table B-7 summarizes the calculated fuel/air mass ratios and fuel mole fractions in air at sea level and at 14,000 feet for the nominal fuel loading (V/L = 274; ~3 kg/m^3) at 40°C, 50°C, and 60°C. This table can be compared directly with Table 4.

Half-filled tank (400 kg/m^3 [V/L = 1.2]). Figure 2 shows a typical chromatogram for a liquid fuel (Base Jet [quarter-scale test #46]), along with a chromatogram of the mixed hydrocarbon standard. The approximately evenly spaced prominent peaks in the liquid fuel represented the normal alkanes, whose retention times matched those for the reference hydrocarbons. The sixteen regression equations -- correlations of mass of hydrocarbon injected with instrument response (e.g., peak area) -- were linear, with correlation coefficient (r^2) values near unity. As was done in the headspace vapor method, each subsection summed GC peak area (5-20) in the liquid method was treated as an individual compound and was used in the appropriate subsection reference standard regression equation to calculate subsection mass (m_i). Each mass was then divided by the molecular weight of the reference hydrocarbon ($[mw]_i$), giving the number of moles (n_i) from which subsection mole fraction was derived. That is,

$$m_i/[mw]_i = n_i \qquad (3)$$

where i = 5,...,20. Then, subsection mole fraction (X_i) was given by

$$X_i = n_i/\Sigma n_{5\text{-}20} \qquad (4)$$

Table 5 lists the subsection mole percent values ($X_i \cdot 100$) for each of the eight fuels. These liquid mole percent values can be used to calculate fuel vapor pressure at any given temperature. For example, Table 6 lists the total vapor pressures calculated for each fuel at

Table 5. Subsection mole percent for liquid ARCO fuel samples.

	Subsection Mole Percent							
Sample	5	6	7	8	9	10	11	12
Base Jet[a]	0.045	0.291	2.30	3.94	6.64	11.5	17.7	18.4
2.5wt% OH	0.110	1.14	7.44	9.02	7.90	10.0	15.4	15.5
97.5wt%	0.018	0.038	0.681	2.46	6.22	12.0	18.6	19.1
95wt%	0.004	0.005	0.154	0.984	4.66	12.3	19.4	19.9
92.5wt%	0.006	--	0.036	0.408	2.81	11.4	20.0	20.6
90wt%	0.005	0.012	0.085	0.235	1.79	9.92	20.7	21.7
87.5wt%	0.005	0.0003	0.003	0.052	0.971	7.84	19.9	21.8
85wt%	0.004	0.0006	0.003	0.013	0.406	5.88	19.9	22.7

	Subsection Mole Percent							
Sample	13	14	15	16	17	18	19	20
Base Jet[a]	15.8	11.8	6.94	3.01	1.18	0.294	0.061	0.040
2.5wt% OH	13.8	9.98	5.95	2.49	0.968	0.182	0.043	0.031
97.5wt%	16.6	12.3	7.25	3.10	1.19	0.290	0.060	0.040
95wt%	17.4	12.9	7.48	3.18	1.26	0.323	0.065	0.033
92.5wt%	18.0	13.3	8.05	3.52	1.33	0.399	0.064	0.044
90wt%	18.4	13.9	8.05	3.45	1.32	0.280	0.068	0.029
87.5wt%	19.3	14.5	8.69	4.09	1.73	0.690	0.246	0.130
85wt%	20.0	15.1	9.02	4.33	1.65	0.664	0.217	0.119

[a] Quarter-scale test #46.

Table 6. Calculated total vapor pressure and average molecular weight for liquid ARCO fuel samples.

	Total Vapor Pressure, mbar			
Sample	40°C[a]	50°C[a]	60°C[b]	Ave Liquid MW
Base Jet	7.91	12.6	19.4	169.1
2.5 wt% OH	20.3	31.2	46.8	160.2
97.5 wt% Btm	4.05	6.74	11.0	171.6
95 wt% Btm	2.34	4.07	6.98	173.8
92.5 wt% Btm	1.68	2.98	5.25	175.9
90 wt% Btm	1.51	2.67	4.73	176.8
87.5 wt% Btm	1.06	1.94	3.55	179.8
85 wt% Btm	0.865	1.60	3.00	181.0

[a] For subsections C_5-C_{12} only.

[b] Base Jet and 2.5 wt% OH: C_5-C_{12} only. Remaining samples: C_5-C_{13}.

40°C, 50°C, and 60°C, along with estimated average molecular weights for the liquids. To obtain the data in Table 6, the saturation vapor pressures for each subsection reference hydrocarbon at each temperature was calculated using the Harlacher equation (Reid et al., 1977), which is valid up to the critical conditions and takes the following form:

$$\text{Ln } P_i^* = A+(B/T)+C\bullet\text{LnT}+(D\bullet P_i^*)/T^2 \qquad (5)$$

where P_i^* *(i = 5,...,20) is* the vapor pressure (torr) and T is the absolute temperature. The terms A, B, C, and D were taken from Appendix A in Reid et al. (1977). Calculation was done by a rapid iteration method using equation solving software. The torr units were converted to mbar by the conversion factor 1.3332 (i.e., mbar = torr•1.3332). Each subsection partial pressure (P_i, i = 5,...,20) was then obtained from the product of the subsection saturation pressure (P_i^*) and subsection liquid mole fraction (X_i = mole%/100) using Raoult's law:

$$P_i = \gamma_i\bullet X_i\bullet P_i^* \qquad (6)$$

For these calculations, it was assumed that the activity coefficient (γ_i) for each component was unity. Subsection mole fraction (X_i) and reference hydrocarbon molecular weight ($[mw]_i$) were used to calculate average liquid molecular weight ($[mw]_{5\text{-}20}$):

$$[mw]_{5\text{-}20} = \Sigma\ (X_i\bullet[mw]_i) \qquad (7)$$

By using the liquid subsection partial pressures (P_i), derived from the subsection mole fractions as discussed above, the vapor composition above each liquid fuel was estimated at 40°C, 50°C, and 60°C. This was done by using a rearranged form of the ideal gas law equation:

$$(n/V)_i = P_i/(R\bullet T\bullet 1013.232) \qquad (8)$$

where $(n/V)_i$ is subsection molar density in the vapor (moles/L), R is the gas constant (0.08205 L-atm/°K•mole), T is absolute temperature, and 1013.232 converts from mbar to atmospheres. This subsection molar density was then used to calculate total vapor mass density ($[g/L]_{5\text{-}20}$):

$$[g/L]_{5\text{-}20} = \Sigma[g/L]_i \qquad (9)$$

where

$$[g/L]_i = (n/V)_i \cdot [mw]_i \quad (10)$$

And, average molecular weight of the total vapor ($[mw_v]_{5\text{-}20}$) was also calculated:

$$[mw_v]_{5\text{-}20} = \Sigma Y_i \cdot [mw]_i \quad (11)$$

and

$$Y_i = (n/V)_i / \Sigma(n/V)_{5\text{-}20} \quad (12)$$

where Y_i is the subsection mole fraction in the vapor.

Table 7 summarizes the results for vapor density (g/m^3) and average vapor molecular weight, and these results are compared with the results derived directly from the characterization of the fuel vapor for subsections C_5-C_{12} (plus C_{13} at 60°C) only. For the average vapor molecular weight, the two sets of results compared within 0.1-3% (ave: 1.2%), 0.4-2% (ave: 1.3%), and 1-2% (ave: 1.7%) at 40°C, 50°C, and 60°C, respectively. The vapor density results compared within 3-29% (ave: 18%), 4-18% (ave: 11%), and 1.5-14% (ave: 6%) at the same respective temperatures. Table 8 lists regressions of vapor pressure vs. temperature derived from liquid characterization. These equations should be compared to the regressions in Table 3 for the half-filled tank (400 kg/m^3). Using the regressions in Tables 3 and 8, vapor pressures were calculated at the flash points of the ARCO fuels. Results are shown in the last two columns of Table 8: "HS-GC", derived from the regressions in Table 3, and "Liquid-GC", derived from the regressions in Table 8. Overall, the two sets of data compared reasonably well. The average difference was 4.8% (range: 1.1-16%), with a median difference of 2.8%. The flash point vapor pressure data in Table 8 can be taken one step further to give the fuel/air mass ratios (FARs) at the flash points. Table 9 summarizes the results for the ARCO fuels, showing that the FARs for headspace and liquid characterizations compared well. The average difference was 5.0% (range: 0-16%), with a median difference of 3.0%. The greatest differences were for the two extremes -- 2.5 wt% OH (10%) and 85 wt% Btm (16%). These differences were due primarily to limits in the headspace vapor method's

Table 7. Comparison of vapor density and average vapor molecular weight derived from vapor and liquid ARCO jet fuel characterization.

		Ave Molecular Wt. (vapor)		Vapor Density, g/m^3	
Sample	Temp., °C	HS-GC[a]	Liquid GC[b]	HS-GC	Liquid GC
Base Jet	40	110.4	108.6	35.4	33.0
2.5 wt% OH		103.8	101.6	81.4	79.1
97.5 wt%		123.4	120.0	21.2	18.7
95 wt%		132.7	131.6	14.5	11.8
92.5 wt%		137.5	137.0	10.7	8.83
90 wt%		138.0	136.4	10.0	7.90
87.5 wt%		143.5	143.6	7.85	5.86
85 wt%		147.4	146.9	6.55	4.88
Base Jet	50	112.6	110.4	54.9	51.6
2.5 wt% OH		105.1	102.8	127.0	119.4
97.5 wt%		124.8	122.0	32.0	30.6
95 wt%		134.6	133.2	21.8	20.2
92.5 wt%		140.1	138.7	18.5	15.4
90 wt%		140.0	138.6	15.7	13.8
87.5 wt%		146.0	145.4	12.6	10.5
85 wt%		149.3	148.6	10.3	8.83
Base Jet	60	113.8	112.2	77.4	78.6
2.5 wt% OH		106.3	103.8	163.2	175.7
97.5 wt%		127.5	124.6	50.7	49.5
95 wt%		138.0	135.6	35.7	34.2
92.5 wt%		143.3	141.4	27.8	26.8
90 wt%		144.5	141.8	27.7	24.2
87.5 wt%		150.7	148.4	21.2	19.0
85 wt%		153.2	151.8	16.8	16.4

[a] Derived from vapor characterization.

[b] Derived from liquid characterization.

Table 8. Flash point and vapor pressure vs. temperature regression curves for liquid ARCO jet fuel samples.

			VP at Flash Point, mbar	
Sample	Flash Point, °F (°C)	VP vs. Temp. Regressions[a]	HS-GC[b]	Liquid-GC
2.5 wt% OH	87 (30.6)	Ln VP = 16.917 - 4352.9 (1/T)	14.4	13.2
Base Jet[c]	114 (45.6)	Ln VP = 17.008 - 4675.9 (1/T)	10.7	10.3
97.5 wt% Btm	132 (55.6)	Ln VP = 18.031 - 5206.5 (1/T)	9.01	8.90
95 wt% Btm	139 (59.4)	Ln VP = 19.038 - 5693.9 (1/T)	6.86	6.74
92.5 wt% Btm	148 (64.4)	Ln VP = 19.480 - 5936.3 (1/T)	6.70	6.59
90 wt% Btm	159 (70.6)	Ln VP = 19.410 - 5948.3 (1/T)	8.53	8.15
87.5 wt% Btm	160 (71.1)	Ln VP = 20.169 - 6296.4 (1/T)	6.42	6.49
85 wt% Btm	165 (73.9)	Ln VP = 20.543 - 6478.0 (1/T)	5.50	6.48

[a] VP = vapor pressure in mbar; T = °K. Regressions derived from liquid characterization.

[b] See Table 3 for regressions derived from vapor characterization (400 kg/m^3 equivalent).

[c] Same as fuel sample from quarter-scale test #46.

Table 9. Fuel/air mass ratios (FARs) for the ARCO fuels at their flash points.

		FAR at Fuel Flash Point	
Sample	Ave. Vapor MW	Liquid-GC[a]	HS-GC[b]
2.5 wt% OH	100.7	0.045	0.050
Base Jet[c]	110.2	0.039	0.040
97.5 wt% Btm	124.2	0.038	0.038
95 wt% Btm	136.5	0.031	0.032
92.5 wt% Btm	143.1	0.032	0.033
90 wt% Btm	144.9	0.040	0.042
87.5 wt% Btm	151.5	0.034	0.033
85 wt% Btm	155.2	0.034	0.029

[a] Derived from liquid characterization.

[b] Derived from vapor characterization.

[c] Liquid-GC: Quarter-scale test #46; HS-GC: Averaged data for fuel samples from quarter-scale tests #42, 46, and 51 (Tables A-1 through A-6).

ability to accurately model the most volatile fuel at 60°C and the least volatile fuel at 40°C (see the following discussion).

Table 10 compares the total fuel vapor pressures, along with percent difference (%Δ), derived from vapor and liquid characterizations. For the 2.5 wt% OH fuel, the somewhat lower vapor-derived value at 60°C was probably due to some flame detector saturation by this rather volatile fuel. Otherwise, the two data sets compared reasonably well overall. There was a trend toward greater differences between the vapor pressures at 40°C, with the vapor-derived values being greater. The information in Table 11 suggests, at the least, a partial explanation as to why this was the case. Liquid mole fractions for subsections C_5-C_{12} are listed for the fuels Base Jet (quarter-scale test #46) and 85 wt% Btm, as examples. The data under "Liquid GC" were taken from the liquid characterization work, while the data under "HS-GC" were calculated from vapor characterization data (i.e., dividing the vapor partial pressure by the saturation pressure). For both fuels, the mole fraction sum for the "HS-GC" data approached that for the "Liquid GC" data only when the temperature for the former fuel was increased. This is believed to be a consequence of the way the headspace instrument responds to higher molecular weight (lower volatility) reference standards below, but near, their saturation vapor densities.

In the ideal situation, as the amount of hydrocarbon is increased in the vapor, instrument response will increase until vapor saturation is reached, where the slope of the instrument response will undergo a sharp change leading to a plateau (area enclosed in the circle in Figure 6). At this point, increasing the amount of hydrocarbon in the closed container will not affect instrument response. In practice with the HS-GC instrument, however, the headspace response seems to follow a curve when the hydrocarbon vapor concentration approaches saturation. This phenomenon is shown in the right-hand portion of Figure 6, along with several lines tangent to this curve at different points. These lines represent regression lines for a hydrocarbon standard near the hydrocarbon's vapor saturation. For example, as the temperature of dodecane standard is lowered from 60°C to

Table 10. Comparison of ARCO jet fuel vapor pressures derived from vapor and liquid characterization.

	ARCO Jet Fuel Vapor Pressure, mbar[a]								
	40°C			50°C			60°C		
Sample	HS-GC	Liquid GC	%Δ	HS-GC	Liquid GC	%Δ	HS-GC	Liquid GC	%Δ
Base Jet	8.34	7.91	5.3	13.1	12.6	3.9	18.8	19.4	3.1
2.5 wt% OH	20.4	20.3	0.5	32.5	31.2	4.1	42.5	46.8	9.6
97.5wt%	4.46	4.05	9.6	6.89	6.74	2.2	11.0	11.0	-0-
95wt%	2.84	2.34	19.3	4.35	4.07	6.6	7.17	6.98	2.7
92.5wt%	2.02	1.68	18.4	3.55	2.98	17.4	5.37	5.25	2.2
90wt%	1.90	1.57	19.0	3.01	2.80	7.2	5.32	4.79	10.5
87.5wt%	1.42	1.06	29.0	2.31	1.94	17.4	3.90	3.55	9.4
85wt%	1.16	0.865	29.1	1.85	1.60	14.5	3.04	3.00	1.3

[a] HS-GC = headspace gas chromatograph. Vapor pressures were derived from fuel vapor characterization.
Liquid GC: Vapor pressures were derived from liquid fuel characterization.

Table 11. Example comparisons of liquid fuel mole fractions derived from vapor and liquid characterization.

Base Jet (quarter-scale test #46):

	Liquid Fuel Mole Fraction			
		HS-GC		
Subsection	Liquid GC	40°C	50°C	60°C
5	4.5×10^{-4}	8.3×10^{-4}	7.2×10^{-4}	6.8×10^{-4}
6	2.9×10^{-3}	2.2×10^{-3}	2.2×10^{-3}	2.2×10^{-3}
7	2.3×10^{-2}	1.8×10^{-2}	1.8×10^{-2}	1.7×10^{-2}
8	3.9×10^{-2}	4.6×10^{-2}	4.7×10^{-2}	4.3×10^{-2}
9	6.6×10^{-2}	8.7×10^{-2}	8.5×10^{-2}	7.6×10^{-2}
10	0.1146	0.1539	0.1476	0.1307
11	0.1768	0.2363	0.2319	0.1925
12	0.1842	0.2517	0.1874	0.1741
Mole Frac. Sum	0.6070	0.7959	0.7198	0.6362

85 wt% Btm:

	Liquid Fuel Mole Fraction			
		HS-GC		
Subsection	Liquid GC	40°C	50°C	60°C
5	4.0×10^{-5}	6.3×10^{-5}	5.2×10^{-5}	3.1×10^{-5}
6	6.0×10^{-6}	–	–	2.6×10^{-6}
7	2.8×10^{-5}	–	–	–
8	1.3×10^{-4}	2.4×10^{-4}	6.0×10^{-5}	9.6×10^{-5}
9	4.1×10^{-3}	5.8×10^{-3}	4.4×10^{-3}	3.5×10^{-3}
10	5.9×10^{-2}	6.4×10^{-2}	5.9×10^{-2}	5.2×10^{-2}
11	0.1988	0.2887	0.2619	0.2300
12	0.2266	0.3344	0.2538	0.2311
Mole Frac. Sum	0.4887	0.6932	0.5792	0.5167

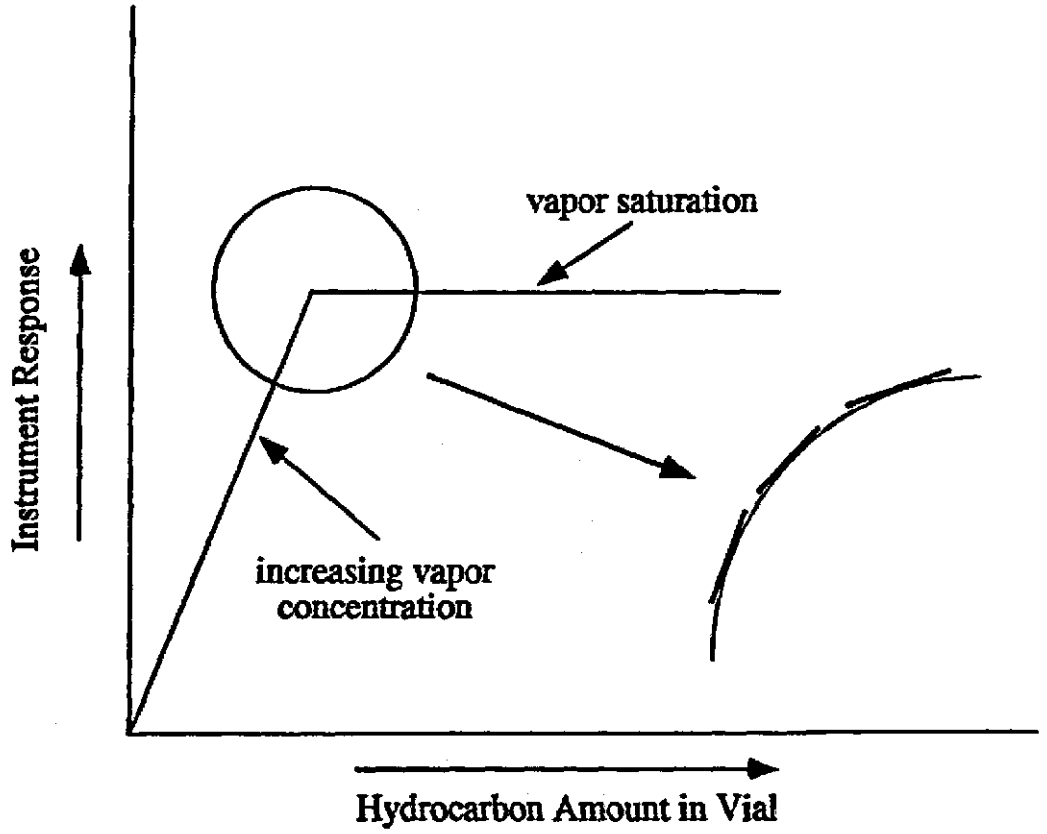

Figure 6. Instrument response vs. hydrocarbon vapor density.

40°C, the slope of the dodecane regression line can decrease by 35-40% as the line moves along the curve toward saturation. Responses for standard reference hydrocarbons C_9, C_{10}, and C_{11} will also be affected in this way by temperature change, with the effect less pronounced at the lower carbon number. The overall result is that, as sample temperature is lowered, higher carbon number subsections (i.e., C_{10}-C_{12}) are biased toward higher mole fraction values.

A possible way to address this problem would be to use the pentane standard regression equation for subsection C_5 for all of the vapor subsections, assuming that the individual components in the higher carbon number subsections are well below their saturation vapor densities. An important justification for using the pentane regression equation is that equal masses of two different n-alkanes will give equivalent responses with the flame ionization detector (responds to moles of carbon); so, the pentane standard can be substituted for the standards hexane-dodecane. Also, compared to dodecane, slopes for the pentane standard regressions at 40°C and 60°C compare within 3-4% (compare with 35-40% for dodecane). The results from applying this approach to the Base Jet fuel vapor (quarter-scale #46) are shown in Table 12, where the liquid fuel mole fractions derived from the C_5 regression equation (again, by dividing the vapor partial pressure by the saturation pressure) are compared to those taken from Table 11. As can be seen, applying the C_5 regression equation to the vapor subsections C_5-C_{12} gave more consistent summed liquid mole fractions and resulted in fuel vapor pressures that compared better with the vapor pressures from the liquid fuel characterization (see Table 10).

Nominal loading (3 kg/m^3 [V/L = 274]). Using the data from the liquid characterization, the molar concentration in the liquid (i.e., mole/L) was calculated for each subsection carbon number. This was simply done by dividing the subsection mass by the reference hydrocarbon molecular weight (equation 3), and then dividing the result by the total volume of sample injected into the analytical instrument. As described earlier, the subsection partial pressures were calculated using each subsection liquid mole fraction

Table 12. Comparison of liquid mole fractions derived from C_5-C_{12} and C_5 only regression equations applied to the vapor characterization of the Base Jet fuel (quarter-scale test #46).

	Liquid Fuel Mole Fraction					
	40°C		50°C		60°C	
Subsection	C_5-C_{12}[a]	C_5[b,c]	C_5-C_{12}	C_5[c]	C_5-C_{12}	C_5[c]
5	8.3×10^{-4}	8.3×10^{-4}	7.2×10^{-4}	7.3×10^{-4}	6.8×10^{-4}	6.8×10^{-4}
6	2.2×10^{-3}	2.2×10^{-3}	2.2×10^{-3}	2.2×10^{-3}	2.2×10^{-3}	2.2×10^{-3}
7	1.8×10^{-2}	1.8×10^{-2}	1.8×10^{-2}	1.8×10^{-2}	1.7×10^{-2}	1.8×10^{-2}
8	4.6×10^{-2}	4.5×10^{-2}	4.7×10^{-2}	4.5×10^{-2}	4.3×10^{-2}	4.4×10^{-2}
9	8.7×10^{-2}	7.9×10^{-2}	8.5×10^{-2}	7.7×10^{-2}	7.6×10^{-2}	7.6×10^{-2}
10	0.1539	0.1258	0.1476	0.1254	0.1307	0.1264
11	0.2363	0.1742	0.2319	0.1833	0.1925	0.1810
12	0.2517	0.1188	0.1874	0.1139	0.1741	0.1414
Mole Frac. Sum	0.7959	0.5638	0.7198	0.5655	0.6362	0.5897

[a] C_5-C_{12} regression equations used.

[b] C_5 regression equation used.

[c] Vapor pressure (mbar): 40°C -- 7.92 (7.91, Table 10)
50°C -- 12.4 (12.6, Table 10)
60°C -- 19.1 (19.4, Table 10)

(Table 5) and saturation vapor pressure, calculated using the Harlacher equation (equation 5). These partial pressures were then converted to their equivalent vapor concentrations (mole/L) using the ideal gas law equation (equation 8).

The resulting liquid and vapor concentration data were used in the following expression:

$$C_G = C^*_L/(K + [V/L]) \quad (13)$$

where C_G is the concentration in the vapor (mole/L), C^*_L is the initial concentration in the liquid (mole/L), K is the hydrocarbon liquid-vapor distribution coefficient, and V/L is the vapor volume-to-liquid volume ratio that would occur in the headspace vial. This expression is known as the "headspace equation" (Ioffe and Vitenberg, 1984b) and it shows that the vapor concentration (C_G) of a hydrocarbon component in the headspace vial depends not only on K, but also on V/L. For a given K, C_G will decrease (increase) as V/L is increased (decreased). With C_G, C^*_L, and V/L (= 1.2 [400 kg/m^3]), it is then possible to solve for K for each subsection carbon number:

$$K = (C^*_L - [C_G\, V/L])/C_G \quad (14)$$

The choice of value for V/L may be somewhat arbitrary, but the value of 1.2 was selected, since this was the ratio used in the headspace method to determine vapor pressures for the half-filled tank. Given C^*_L, K, and V/L (= 274), C_G was then calculated for each hydrocarbon subsection under nominal loading:

$$C_G\ (\text{nom. load}) = C^*_L/(K + 274) \quad (15)$$

Table 13 compares measured (i.e., headspace) vapor pressures for the ARCO fuels at V/L = 274 (~3 kg/m^3) with calculated pressures derived using the method just described. The two sets of data compare reasonably well. The average difference was 6.4% (range: 0.5-15%), with a median difference of 6.2%. Table 14 is a compilation of subsection distribution coefficients for the ARCO fuels. Since the distribution coefficient (K) is proportional to C^*_L/C_G, the higher the value for K, the more the distribution favors the condensed, liquid phase. Finally, Table 15 lists regressions of vapor pressure vs.

Table 13. Measured and calculated vapor pressures for the ARCO jet fuels under nominal loading conditions (V/L = 274 [~3 kg/m^3]).

		Vapor Pressure, mbar		
Sample	Method	40°C	50°C	60°C[a]
Base Jet (#46)	Measured[b]	5.72	8.54	12.2
	Calculated[c]	6.09	9.17	13.4
2.5 wt% OH	Measured	12.7	19.4	27.3
	Calculated	14.7	20.9	28.8
97.5 wt% Btm	Measured	3.08	5.04	8.35
	Calculated	3.48	5.62	8.88
95 wt% Btm	Measured	2.19	3.46	6.19
	Calculated	2.18	3.72	6.24
92.5 wt% Btm	Measured	1.66	2.62	5.02
	Calculated	1.57	2.77	4.83
90 wt% Btm	Measured	1.40	2.18	4.35
	Calculated	1.39	2.44	4.28
87.5 wt% Btm	Measured	1.11	1.71	3.29
	Calculated	1.00	1.82	3.35
85 wt% Btm	Measured	0.940	1.49	2.94
	Calculated	0.819	1.52	2.85

[a] For samples 97.5 wt%-85 wt%, listed vapor pressures are for subsections C_5-C_{13}.

[b] Measured using HS-GC method at V/L = 274 (0.08 mL fuel in 22 mL vial).

[c] Calculated using the headspace equation (see text for explanation):

$$C_G = C^*_L/(K + [V/L])$$

Table 14. Liquid-vapor hydrocarbon distribution coefficients for the ARCO jet fuels.

		Subsection Hydrocarbon Distribution Coefficient (K)[a]								
Fuel	Temp., °C	5	6	7	8	9	10	11	12	13
Base Jet (46)	40	79.2	264	846	2.61E+03	8.03E+03	2.32E+04	6.78E+04	1.95E+05	4.69E+05
	50	57.9	187	563	1.65E+03	4.76E+03	1.31E+04	3.65E+04	9.94E+04	2.28E+05
	60	43.1	134	386	1.08E+03	2.94E+03	7.82E+03	2.03E+04	5.31E+04	1.51E+05
2.5 wt% OH	40	83.5	278	892	2.75E+03	8.46E+03	2.44E+04	7.15E+04	2.06E+05	4.94E+05
	50	61.1	197	594	1.74E+03	5.02E+03	1.38E+04	3.84E+04	1.05E+05	2.40E+05
	60	45.5	141	407	1.13E+03	3.10E+03	8.25E+03	2.14E+04	5.60E+04	1.59E+05
97.5wt%Btm	40	77.9	260	833	2.57E+03	7.90E+03	2.28E+04	6.68E+04	1.92E+05	4.62E+05
	50	57.0	184	554	1.62E+03	4.69E+03	1.29E+04	3.59E+04	9.78E+04	2.24E+05
	60	42.4	132	380	1.06E+03	2.90E+03	7.70E+03	2.00E+04	5.23E+04	1.49E+05
95wt%Btm	40	76.9	257	823	2.54E+03	7.80E+03	2.25E+04	6.60E+04	1.90E+05	4.56E+05
	50	56.2	181	547	1.60E+03	4.63E+03	1.28E+04	3.54E+04	9.66E+04	2.22E+05
	60	41.8	130	375	1.05E+03	2.86E+03	7.60E+03	1.98E+04	5.16E+04	1.47E+05
92.5wt%Btm	40	76.0	–	813	2.50E+03	7.71E+03	2.22E+04	6.52E+04	1.87E+05	4.50E+05
	50	55.5	–	541	1.58E+03	4.57E+03	1.26E+04	3.50E+04	9.54E+04	2.19E+05
	60	41.3	–	371	1.03E+03	2.83E+03	7.51E+03	1.95E+04	5.10E+04	1.45E+05
90wt%Btm	40	75.6	252	809	2.49E+03	7.67E+03	2.21E+04	6.48E+04	1.86E+05	4.48E+05
	50	55.2	178	538	1.57E+03	4.55E+03	1.25E+04	3.48E+04	9.50E+04	2.18E+05
	60	41.1	128	369	1.03E+03	2.81E+03	7.48E+03	1.94E+04	5.08E+04	1.44E+05
87.5wt%Btm	40	74.3	248	795	2.45E+03	7.54E+03	2.18E+04	6.38E+04	1.83E+05	4.40E+05
	50	54.3	175	529	1.55E+03	4.47E+03	1.23E+04	3.42E+04	9.34E+04	2.14E+05
	60	40.4	126	363	1.01E+03	2.77E+03	7.35E+03	1.91E+04	4.99E+04	1.42E+05
85wt%Btm	40	73.8	246	790	2.43E+03	7.49E+03	2.16E+04	6.33E+04	1.82E+05	4.38E+05
	50	53.9	174	525	1.54E+03	4.44E+03	1.22E+04	3.40E+04	9.27E+04	2.13E+05
	60	40.1	125	360	1.00E+03	2.75E+03	7.30E+03	1.90E+04	4.96E+04	1.41E+05

[a] $K \propto C^{*}_{L}/C_{G}$, where C^{*}_{L} is the initial concentration in the liquid and C_{G} is the vapor concentration at equilibrium.

Table 15. Comparison of vapor pressure vs. temperature regressions derived from liquid and vapor characterization for the ARCO jet fuel samples at nominal loading (3 kg/m^3).

		Vapor Pressure vs. Temperature Regressions[a]	
Sample	Flash Point, °F (°C)	Liquid-GC	HS-GC[b]
2.5 wt% OH	87 (30.6)	Ln VP = 13.889 - 3505.4 (1/T)	Ln VP = 15.303 - 3991.3 (1/T)
Base Jet[c]	114 (45.6)	Ln VP = 14.939 - 4110.1 (1/T)	Ln VP = 14.680 - 4053.3 (1/T)
97.5 wt% Btm	132 (55.6)	Ln VP = 16.842 - 4881.5 (1/T)	Ln VP = 17.716 - 5195.1 (1/T)
95 wt% Btm	139 (59.4)	Ln VP = 18.284 - 5479.8 (1/T)	Ln VP = 18.031 - 5406.3 (1/T)
92.5 wt% Btm	148 (64.4)	Ln VP = 19.154 - 5855.2 (1/T)	Ln VP = 18.856 - 5754.7 (1/T)
90 wt% Btm	159 (70.6)	Ln VP = 19.159 - 5897.2 (1/T)	Ln VP = 19.118 - 5892.9 (1/T)
87.5 wt% Btm	160 (71.1)	Ln VP = 20.113 - 6297.8 (1/T)	Ln VP = 18.109 - 5648.5 (1/T)
85 wt% Btm	165 (73.9)	Ln VP = 20.546 - 6496.0 (1/T)	Ln VP = 18.839 - 5928.7 (1/T)

[a] VP = vapor pressure in mbar; T = °K.

[b] Data taken from Table 3.

[c] Liquid-GC: Quarter-scale test #46; HS-GC: Averaged data for fuel samples from quarter-scale tests #42, 46, and 51 (Tables A-1 through A-6).

temperature for nominal loading (3 kg/m^3) using the data in Table 13 ("Calculated"). Regressions from Table 3 are included for comparison ("HS-GC").

Summary

1. For the ARCO fuels reformulated for flash point, there was an inverse relationship between vapor pressure and flash point temperature (i.e., the fuel with the highest vapor pressure had the lowest flash point).

2. The commercial grade ARCO and Reno (Exxon) fuels had different formulations -- component distribution favored the lighter hydrocarbons in the ARCO fuel -- but both fuels had essentially the same saturation vapor pressures (within 1-7%) at the test temperatures.

3. The two fuels used in the Marana, AZ, ground tests (#1, #3) were similar to the Reno fuel in formulation, but had about a 15-20% lower vapor pressure, which might have been due to some weathering of the fuel in the warm (>40°C) center wing tank of a 747 aircraft.

4. Vapor densities for all of the commercial grade jet fuels (quarter-scale test samples #42, 46, 51, and Marana, AZ, ground test samples #1 and 3) either equaled or exceeded the lower flammability limit (fuel/air mass ratio = 0.038) for nominal fuel loading (V/L = 274 [~3 kg/m^3]) at 40°C and 14,000 foot altitude.

5. All but two of the reformulated flash point ARCO fuels equaled or exceeded the lower flammability limit at 60°C for 14,000 feet. The exceptions -- fuels 87.5 wt% Btm and 85 wt% Btm -- were less than the limit at 60°C. Fuel 97.5 wt% Btm exceeded the limit at 50°C, and fuel 2.5 wt% OH exceeded the limit at sea level and 40°C.

6. Overall, liquid characterization gave results for the half-filled tank situation that were essentially equivalent to the results from vapor characterization. But, liquid characterization better represented the contribution to fuel vapor composition from the higher molecular weight components. This led to the modification to the vapor method involving the use of the C_5 reference standard regression for all of the vapor subsections (i.e., C_5-C_{13}). For

example, for the Base Jet fuel (quarter-scale test #46), use of the C_5 reference standard only led to fuel vapor pressures of 7.92, 12.4, and 19.1 mbar at 40°C, 50°C, and 60°C, respectively. These results compared well with the values derived from liquid characterization of 7.91, 12.6, and 19.4 mbar at the same respective temperatures (see Tables 10 and 12).

7. Furthermore, liquid characterization also gave results for the nominal loading situation that compared well with the results from vapor characterization.

8. Using the techniques described in this report, it is possible to characterize (model) a complex hydrocarbon mixture under any specified set of conditions. For example, using Raoult's law, the liquid characterization results can be used to calculate fuel vapor pressure at any given temperature, if the saturation vapor pressures for the reference hydrocarbons at those temperatures are known.

References

Ioffe, B.V., and A.G. Vitenberg. **1984a.** *Head-Space Analysis and Related Methods in Gas Chromatography.* (Translated from the Russian by I.A. Mamantov). John Wiley & Sons: New York, pp. 94-96.

Ioffe, B.V., and A.G. Vitenberg. **1984b.** *Head-Space Analysis and Related Methods in Gas Chromatography.* (Translated from the Russian by I.A. Mamantov). John Wiley & Sons: New York, pg. 26.

Reid, R.C.; J.M Prausnitz; T.K. Sherwood. **1977.** *The Properties of Gases and Liquids.* McGraw-Hill: New York, pp. 629-665.

Sagebiel, J.C. **1998.** *Analysis of Vapor Samples Collected from the Center Wing Tank of a Boeing 747-100 Aircraft during Ground Tests.* Draft Final Report to the National Transportation Safety Board, October.

Shepherd, J.E.; C.D. Nuyt; J.J. Lee. **2000.** *Flash Point and Chemical Composition of Aviation Kerosene (Jet A).* Explosion Dynamics Report FM99-4, California Institute of Technology, May 26.

Woodrow, J.E., and J.N. Seiber. **1988.** Vapor-pressure measurement of complex hydrocarbon mixtures by headspace gas chromatography. *Journal of Chromatography,* 455:53-65.

Woodrow, J.E., and J.N. Seiber. **1989.** *Evaluation of a Method for Determining Vapor Pressures of Petroleum Mixtures by Headspace Gas Chromatography.* Final Report to the California Air Resources Board (Contract #A6-178-32), September.

Woodrow, J.E., and J.N. Seiber. **1997.** *The Laboratory Characterization of Jet Fuel Vapor under Simulated Flight Conditions.* Final Report to the National Transportation Safety Board (Order No. NTSB12-97-0255), November.

Appendix A

Headspace GC results for the ARCO fuel samples and the Marana, AZ, ground test fuel samples

Table A-1. Headspace GC results for ARCO samples at 40°C (10 mL [V/L = 1.2]).

	Subsection Partial Pressure, mbar								
Sample	5	6	7	8	9	10	11	12	Total Pressure, mbar
2.5% OH	1.83	3.24	7.84	4.78	1.56	0.649	0.380	0.148	20.4±0.5
97.5%	0.344	0.125	0.568	0.926	1.03	0.799	0.492	0.174	4.46±0.06
95%	0.143	0.048	0.151	0.362	0.682	0.793	0.496	0.164	2.84±0.06
92.5%	0.141	0.002	0.025	0.158	0.400	0.666	0.464	0.165	2.02±0.07
90%	0.100	0.030	0.086	0.136	0.280	0.584	0.501	0.179	1.90±0.07
87.5%	0.107	0.002	0.002	0.024	0.152	0.456	0.500	0.182	1.42±0.02
85%	0.073	--	--	0.010	0.082	0.310	0.485	0.198	1.16±0.01
#42	1.06	0.827	2.22	1.89	1.20	0.753	0.407	0.150	8.51±0.08
#46	0.962	0.818	2.20	1.88	1.19	0.745	0.397	0.149	8.34±0.11
#51	0.943	0.791	2.18	1.77	1.15	0.735	0.418	0.147	8.13±0.28

	Subsection Mole Percent								
Sample	5	6	7	8	9	10	11	12	Ave MW
2.5% OH	8.96	15.9	38.4	23.4	7.64	3.18	1.86	0.724	103.8
97.5%	7.72	2.80	12.7	20.8	23.1	17.9	11.0	3.90	123.4
95%	5.04	1.69	5.32	12.8	24.0	27.9	17.5	5.78	132.7
92.5%	6.98	0.099	1.24	7.82	19.8	33.0	23.0	8.16	137.5
90%	5.27	1.58	4.54	7.17	14.8	30.8	26.4	9.44	138.0
87.5%	7.51	0.140	0.140	1.68	10.7	32.0	35.1	12.8	143.5
85%	6.30	--	--	0.864	7.08	26.8	41.9	17.1	147.4
#42	12.5	9.72	26.1	22.2	14.1	8.85	4.78	1.76	110.1
#46	11.5	9.81	26.4	22.5	14.3	8.93	4.76	1.79	110.4
#51	11.6	9.72	26.8	21.8	14.1	9.04	5.14	1.81	110.6

Table A-1, cont.

	Subsection Vapor Density, g/m^3								
Sample	5	6	7	8	9	10	11	12	Total Density, g/m^3
2.5% OH	5.07	10.7	30.2	21.0	7.69	3.55	2.28	0.969	81.4
97.5%	0.954	0.414	2.19	4.06	5.08	4.37	2.96	1.14	21.2
95%	0.396	0.159	0.581	1.59	3.36	4.34	2.98	1.07	14.5
92.5%	0.391	0.007	0.096	0.694	1.97	3.64	2.79	1.08	10.7
90%	0.277	0.099	0.331	0.597	1.38	3.19	3.01	1.17	10.0
87.5%	0.297	0.007	0.008	0.105	0.749	2.49	3.00	1.19	7.85
85%	0.202	--	--	0.044	0.404	1.69	2.91	1.30	6.55
#42	2.94	2.74	8.55	8.30	5.91	4.12	2.44	0.982	36.0
#46	2.67	2.71	8.47	8.25	5.86	4.07	2.38	0.975	35.4
#51	2.61	2.62	8.39	7.77	5.67	4.02	2.51	0.962	34.6

Table A-2. Headspace GC results for ARCO samples at 40°C (0.08 mL [V/L = 274]).

	Subsection Partial Pressure, mbar								
Sample	5	6	7	8	9	10	11	12	Total Pressure, mbar
2.5% OH	0.309	1.47	5.10	3.56	1.24	0.547	0.341	0.138	12.7±0.30
97.5%	0.058	0.069	0.356	0.658	0.775	0.632	0.373	0.162	3.08±0.10
95%	0.031	0.035	0.103	0.266	0.537	0.629	0.426	0.165	2.19±0.05
92.5%	0.020	--	0.016	0.128	0.347	0.558	0.427	0.166	1.66±0.05
90%	0.010	0.013	0.052	0.099	0.211	0.458	0.404	0.151	1.40±0.03
87.5%	0.017	--	0.029	0.042	0.114	0.352	0.400	0.157	1.11±0.05
85%	0.016	--	--	0.035	0.066	0.253	0.401	0.172	0.94±0.06
#42	0.124	0.400	1.51	1.47	1.00	0.655	0.369	0.132	5.66±0.10
#46	0.120	0.398	1.52	1.46	1.01	0.678	0.385	0.150	5.72±0.20
#51	0.112	0.368	1.42	1.36	0.968	0.658	0.396	0.155	5.44±0.02

	Subsection Mole Percent								
Sample	5	6	7	8	9	10	11	12	Ave MW
2.5% OH	2.43	11.6	40.1	28.0	9.76	4.30	2.68	1.09	108.6
97.5%	1.88	2.24	11.5	21.3	25.1	20.5	12.1	5.25	128.4
95%	1.41	1.60	4.70	12.1	24.5	28.7	19.4	7.53	136.3
92.5%	1.20	--	0.963	7.70	20.9	33.6	25.7	9.99	142.4
90%	0.715	0.930	3.72	7.08	15.1	32.8	28.9	10.8	142.7
87.5%	1.53	--	2.61	3.78	10.3	31.7	36.0	14.1	146.6
85%	1.70	--	--	3.71	7.00	26.8	42.5	18.2	150.0
#42	2.19	7.07	26.7	26.0	17.7	11.6	6.52	2.33	117.4
#46	2.10	6.96	26.6	25.5	17.6	11.8	6.73	2.62	117.8
#51	2.06	6.77	26.1	25.0	17.8	12.1	7.28	2.85	118.3

Table A-2, cont.

Sample	Subsection Vapor Density, g/m^3								Total Density, g/m^3
	5	6	7	8	9	10	11	12	
2.5% OH	0.857	4.87	19.6	15.6	6.11	2.99	2.05	0.903	53.0
97.5%	0.161	0.228	1.37	2.89	3.82	3.46	2.24	1.06	15.2
95%	0.086	0.116	0.396	1.17	2.65	3.44	2.56	1.08	11.5
92.5%	0.055	--	0.062	0.562	1.71	3.05	2.56	1.09	9.09
90%	0.028	0.043	0.200	0.434	1.04	2.50	2.43	0.988	7.66
87.5%	0.047	--	0.112	0.184	0.562	1.92	2.40	1.03	6.26
85%	0.044	--	--	0.154	0.325	1.38	2.41	1.12	5.43
#42	0.344	1.32	5.81	6.45	4.93	3.58	2.22	0.864	25.5
#46	0.333	1.32	5.85	6.41	4.98	3.71	2.31	0.982	25.9
#51	0.310	1.22	5.47	5.97	4.77	3.60	2.38	1.01	24.7

Table A-3. Headspace GC results for ARCO samples at 50°C (10 mL [V/L = 1.2]).

	Subsection Partial Pressure, mbar								
Sample	5	6	7	8	9	10	11	12	Total Pressure, mbar
2.5% OH	2.50	4.99	11.6	8.51	2.82	1.15	0.666	0.224	32.5±0.3
97.5%	0.407	0.142	0.808	1.52	1.71	1.29	0.745	0.264	6.89±0.06
95%	0.161	0.009	0.173	0.559	1.14	1.30	0.764	0.240	4.35±0.05
92.5%	0.147	--	0.036	0.229	0.688	1.26	0.909	0.277	3.55±0.15
90%	0.116	0.040	0.114	0.177	0.435	1.00	0.866	0.262	3.01±0.05
87.5%	0.119	--	--	0.034	0.220	0.728	0.926	0.286	2.31±0.11
85%	0.082	--	--	0.004	0.105	0.516	0.838	0.302	1.85±0.03
#42	1.24	1.16	3.42	3.09	2.00	1.28	0.748	0.243	13.2±0.2
#46	1.15	1.16	3.41	3.10	2.01	1.29	0.742	0.223	13.1±0.3
#51	1.17	1.16	3.50	3.02	2.03	1.31	0.770	0.255	13.2±0.03

	Subsection Mole Percent								
Sample	5	6	7	8	9	10	11	12	Ave MW
2.5% OH	7.70	15.4	35.7	26.2	8.69	3.54	2.05	0.690	105.1
97.5%	5.91	2.06	11.7	22.1	24.8	18.7	10.8	3.83	124.8
95%	3.70	0.207	3.98	12.9	26.2	29.9	17.6	5.52	134.6
92.5%	4.14	--	1.02	6.46	19.4	35.5	25.6	7.81	140.1
90%	3.85	1.33	3.79	5.88	14.4	33.2	28.8	8.70	140.0
87.5%	5.14	--	--	1.47	9.51	31.5	40.0	12.4	146.0
85%	4.44	--	--	0.216	5.68	27.9	45.4	16.4	149.3
#42	9.41	8.80	26.0	23.4	15.2	9.71	5.67	1.84	112.5
#46	8.79	8.86	26.1	23.7	15.4	9.86	5.67	1.70	112.6
#51	8.85	8.78	26.5	22.8	15.4	9.91	5.83	1.93	112.8

Table A-3, cont.

Sample	Subsection Vapor Density, g/m^3								Total Density, g/m^3
	5	6	7	8	9	10	11	12	
2.5% OH	6.72	16.0	43.3	36.2	13.5	6.09	3.88	1.42	127
97.5%	1.09	0.456	3.01	6.46	8.17	6.83	4.34	1.67	32.0
95%	0.432	0.029	0.645	2.38	5.44	6.89	4.45	1.52	21.8
92.5%	0.395	--	0.134	0.974	3.28	6.68	5.29	1.76	18.5
90%	0.312	0.128	0.425	0.753	2.08	5.30	5.04	1.66	15.7
87.5%	0.320	--	--	0.145	1.05	3.86	5.39	1.81	12.6
85%	0.220	--	--	0.017	0.501	2.73	4.88	1.92	10.3
#42	3.33	3.72	12.8	13.1	9.55	6.78	4.35	1.54	55.2
#46	3.09	3.72	12.7	13.2	9.60	6.83	4.32	1.41	54.9
#51	3.14	3.72	13.1	12.8	9.69	6.94	4.48	1.62	55.5

Table A-4. Headspace GC results for ARCO samples at 50°C (0.08 mL [V/L = 274]).

	Subsection Partial Pressure, mbar								
Sample	5	6	7	8	9	10	11	12	Total Pressure, mbar
2.5% OH	0.331	1.90	7.16	6.02	2.21	0.963	0.582	0.214	19.4±0.7
97.5%	0.052	0.060	0.499	1.12	1.37	1.07	0.633	0.233	5.04±0.14
95%	0.014	0.003	0.110	0.412	0.908	1.09	0.684	0.243	3.46±0.06
92.5%	0.008	--	0.022	0.158	0.504	0.964	0.721	0.248	2.62±0.04
90%	0.007	0.015	0.068	0.121	0.317	0.725	0.696	0.230	2.18±0.08
87.5%	0.004	--	--	0.023	0.166	0.560	0.730	0.231	1.71±0.11
85%	0.011	--	--	0.005	0.081	0.428	0.702	0.262	1.49±0.01
#42	0.124	0.473	2.08	2.33	1.67	1.13	0.675	0.210	8.69±0.12
#46	0.115	0.461	2.04	2.28	1.64	1.10	0.672	0.228	8.54±0.28
#51	0.111	0.446	2.03	2.15	1.60	1.10	0.669	0.231	8.34±0.21

	Subsection Mole Percent								
Sample	5	6	7	8	9	10	11	12	Ave MW
2.5% OH	1.71	9.80	36.9	31.1	11.4	4.97	3.00	1.10	110.4
97.5%	1.03	1.19	9.91	22.2	27.2	21.2	12.6	4.62	129.7
95%	0.404	0.087	3.18	11.9	26.2	31.5	19.7	7.01	138.3
92.5%	0.305	--	0.838	6.02	19.2	36.7	27.5	9.45	143.9
90%	0.321	0.688	3.12	5.55	14.5	33.3	31.9	10.6	144.2
87.5%	0.233	--	--	1.34	9.68	32.7	42.6	13.5	150.2
85%	0.739	--	--	0.336	5.44	28.7	47.1	17.6	152.3
#42	1.43	5.45	24.0	26.8	19.2	13.0	7.77	2.42	119.8
#46	1.35	5.40	23.9	26.7	19.2	12.9	7.87	2.67	119.9
#51	1.33	5.35	24.3	25.8	19.2	13.2	8.02	2.77	120.1

Table A-4, cont.

Sample	Subsection Vapor Density, g/m^3								Total Density, g/m^3
	5	6	7	8	9	10	11	12	
2.5% OH	0.889	6.10	26.7	25.6	10.6	5.10	3.39	1.36	79.7
97.5%	0.140	0.192	1.86	4.76	6.54	5.67	3.68	1.48	24.3
95%	0.038	0.010	0.410	1.75	4.34	5.77	3.98	1.54	17.8
92.5%	0.021	--	0.082	0.672	2.41	5.11	4.20	1.57	14.1
90%	0.019	0.048	0.254	0.515	1.51	3.84	4.05	1.46	11.7
87.5%	0.011	--	--	0.098	0.793	2.97	4.25	1.46	9.58
85%	0.030	--	--	0.021	0.387	2.27	4.08	1.66	8.45
#42	0.333	1.52	7.76	9.91	7.98	5.99	3.93	1.33	38.7
#46	0.309	1.48	7.61	9.70	7.83	5.83	3.91	1.45	38.1
#51	0.298	1.43	7.57	9.14	7.64	5.83	3.89	1.46	37.3

Table A-5. Headspace GC results for ARCO samples at 60°C (10 mL [V/L = 1.2]).

	Subsection Partial Pressure, mbar									
Sample	5	6	7	8	9	10	11	12	13	Total Pressure, mbar
2.5% OH	3.10	6.16	14.7	11.1	4.19	1.77	1.07	0.388	--	42.5±0.9
97.5%	0.512	0.202	1.24	2.32	2.67	2.10	1.33	0.478	0.151	11.0±0.1
95%	0.163	0.016	0.255	0.825	1.73	2.13	1.39	0.504	0.155	7.17±0.22
92.5%	0.161	0.003	0.047	0.300	0.955	1.85	1.40	0.503	0.149	5.37±0.13
90%	0.128	0.053	0.192	0.265	0.657	1.60	1.57	0.651	0.202	5.32±0.17
87.5%	0.109	0.002	0.002	0.044	0.305	1.12	1.55	0.586	0.187	3.90±0.29
85%	0.067	0.002	--	0.010	0.136	0.787	1.35	0.527	0.160	3.04±0.22
#42	1.57	1.64	4.84	4.47	2.98	1.98	1.18	0.399	--	19.1±0.7
#46	1.46	1.63	4.82	4.46	2.98	1.96	1.13	0.397	--	18.8±0.6
#51	1.49	1.62	4.78	4.42	2.96	1.97	1.17	0.391	--	18.8±0.8

	Subsection Mole Percent									
Sample	5	6	7	8	9	10	11	12	13	Ave MW
2.5% OH	7.30	14.5	34.6	26.1	9.86	4.17	2.52	0.913	--	106.3
97.5%	4.65	1.84	11.3	21.1	24.3	19.1	12.1	4.34	1.37	127.5
95%	2.27	0.223	3.56	11.5	24.1	29.7	19.4	7.03	2.16	138.0
92.5%	3.00	0.056	0.876	5.59	17.8	34.5	26.1	9.37	2.78	143.3
90%	2.41	0.997	3.61	4.98	12.4	30.1	29.5	12.2	3.80	144.5
87.5%	2.79	0.051	0.051	1.13	7.81	28.7	39.7	15.0	4.79	150.7
85%	2.20	0.066	--	0.329	4.48	25.9	44.4	17.3	5.26	153.2
#42	8.24	8.60	25.4	23.4	15.6	10.4	6.19	2.09	--	113.6
#46	7.75	8.65	25.6	23.7	15.8	10.4	6.00	2.11	--	113.8
#51	7.92	8.62	25.4	23.5	15.7	10.5	6.22	2.08	--	113.8

Table A-5, cont.

	Subsection Vapor Density, g/m^3									
Sample	5	6	7	8	9	10	11	12	13	Total Density, g/m^3
2.5% OH	8.08	19.2	53.2	45.8	19.4	9.10	6.04	2.39	--	163.2
97.5%	1.33	0.629	4.49	9.57	12.4	10.8	7.51	2.94	1.00	50.7
95%	0.425	0.050	0.923	3.40	8.01	10.9	7.85	3.10	1.03	35.7
92.5%	0.420	0.009	0.170	1.24	4.42	9.51	7.90	3.09	0.992	27.8
90%	0.334	0.165	0.695	1.09	3.04	8.22	8.86	4.00	1.34	27.7
87.5%	0.284	0.006	0.007	0.182	1.41	5.76	8.75	3.60	1.24	21.2
85%	0.174	0.006	--	0.041	0.630	4.04	7.62	3.24	1.06	16.8
#42	4.09	5.10	17.5	18.4	13.8	10.2	6.66	2.45	--	78.2
#46	3.80	5.07	17.4	18.4	13.8	10.1	6.38	2.44	--	77.4
#51	3.88	5.04	17.3	18.2	13.7	10.1	6.60	2.40	--	77.3

Table A-6. Headspace GC results for ARCO samples at 60°C (0.08 mL [V/L = 274]).

	Subsection Partial Pressure, mbar									
Sample	5	6	7	8	9	10	11	12	13	Total Pressure, mbar
2.5% OH	0.356	2.43	9.36	8.58	3.54	1.63	1.01	0.385	--	27.3±0.8
97.5%	0.044	0.067	0.704	1.66	2.14	1.85	1.23	0.481	0.171	8.35±0.32
95%	0.009	0.003	0.172	0.616	1.45	1.88	1.31	0.555	0.191	6.19±0.29
92.5%	0.010	--	0.030	0.236	0.829	1.72	1.42	0.591	0.189	5.02±0.10
90%	0.007	0.019	0.119	0.200	0.534	1.35	1.35	0.556	0.212	4.35±0.28
87.5%	0.006	--	--	0.030	0.250	0.986	1.32	0.518	0.176	3.29±0.12
85%	--	--	--	0.007	0.117	0.714	1.30	0.600	0.197	2.94±0.10
#42	0.133	0.581	2.74	3.26	2.47	1.72	1.03	0.385	--	12.3±0.2
#46	0.126	0.566	2.70	3.22	2.45	1.72	1.04	0.391	--	12.2±0.4
#51	0.116	0.559	2.65	3.16	2.42	1.73	1.08	0.400	--	12.1±0.4

	Subsection Mole Percent									
Sample	5	6	7	8	9	10	11	12	13	Ave MW
2.5% OH	1.30	8.90	34.3	31.4	13.0	5.97	3.70	1.41	--	112.2
97.5%	0.527	0.803	8.43	19.9	25.6	22.2	14.7	5.76	2.05	133.2
95%	0.145	0.048	2.78	9.96	23.4	30.4	21.2	8.97	3.09	141.7
92.5%	0.199	--	0.597	4.70	16.5	34.2	28.2	11.8	3.76	147.0
90%	0.161	0.437	2.74	4.60	12.3	31.1	31.1	12.8	4.88	147.9
87.5%	0.182	--	--	0.913	7.61	30.0	40.2	15.8	5.36	153.2
85%	--	--	--	0.238	3.99	24.3	44.3	20.4	6.71	156.3
#42	1.08	4.72	22.2	26.5	20.0	14.0	8.36	3.12	--	121.3
#46	1.03	4.63	22.1	26.4	20.1	14.1	8.52	3.20	--	121.5
#51	0.957	4.61	21.9	26.1	20.0	14.3	8.91	3.30	--	121.9

Table A-6, cont.

	Subsection Vapor Density, g/m^3									
Sample	5	6	7	8	9	10	11	12	13	Total Density, g/m^3
2.5% OH	0.928	7.56	33.9	35.4	16.4	8.38	5.70	2.37	--	110.6
97.5%	0.115	0.208	2.55	6.85	9.91	9.51	6.94	2.96	1.14	40.2
95%	0.023	0.009	0.622	2.54	6.72	9.66	7.40	3.41	1.27	31.6
92.5%	0.026	--	0.109	0.974	3.84	8.84	8.02	3.64	1.26	26.7
90%	0.018	0.059	0.431	0.825	2.47	6.94	7.62	3.42	1.41	23.2
87.5%	0.016	--	--	0.124	1.16	5.07	7.45	3.19	1.17	18.2
85%	--	--	--	0.029	0.542	3.67	7.34	3.69	1.31	16.6
#42	0.346	1.81	9.92	13.4	11.4	8.84	5.81	2.37	--	54.0
#46	0.328	1.76	9.77	13.3	11.3	8.84	5.87	2.40	--	53.6
#51	0.302	1.74	9.59	13.0	11.2	8.89	6.10	2.46	--	53.3

Table A-7. Headspace GC results for the ground test fuel samples at 40°C (10 mL [V/L = 1.2]).

	Subsection Partial Pressure, mbar								
Sample	5	6	7	8	9	10	11	12	Total Pressure, mbar
#1	0.462	0.286	0.871	1.60	1.83	1.18	0.461	0.142	6.83±0.17
#3	0.492	0.301	0.876	1.55	1.78	1.18	0.476	0.135	6.79±0.09

	Subsection Mole Percent								
Sample	5	6	7	8	9	10	11	12	Ave MW
#1	6.76	4.19	12.7	23.4	26.8	17.3	6.75	2.08	121.0
#3	7.24	4.43	12.9	22.8	26.2	17.4	7.01	1.99	120.7

	Subsection Vapor Density, g/m^3								
Sample	5	6	7	8	9	10	11	12	Total Density, g/m^3
#1	1.28	0.947	3.35	7.02	9.02	6.45	2.77	0.929	31.8
#3	1.36	0.997	3.37	6.80	8.77	6.45	2.86	0.884	31.5

Table A-8. Headspace GC results for the ground test fuel samples at 40°C (0.08 mL [V/L = 274]).

	Subsection Partial Pressure, mbar								
Sample	5	6	7	8	9	10	11	12	Total Pressure, mbar
#1	0.069	0.132	0.570	1.22	1.49	1.01	0.425	0.146	5.06±0.20
#3	0.077	0.142	0.590	1.22	1.48	1.05	0.456	0.144	5.16±0.04

	Subsection Mole Percent								
Sample	5	6	7	8	9	10	11	12	Ave MW
#1	1.36	2.61	11.3	24.1	29.4	20.0	8.40	2.88	126.2
#3	1.49	2.75	11.4	23.6	28.7	20.4	8.84	2.79	126.2

	Subsection Vapor Density, g/m^3								
Sample	5	6	7	8	9	10	11	12	Total Density, g/m^3
#1	0.191	0.437	2.19	5.36	7.34	5.52	2.55	0.956	24.5
#3	0.213	0.470	2.27	5.36	7.29	5.74	2.74	0.942	25.0

Table A-9. Headspace GC results for the ground test fuel samples at 50°C (10 mL [V/L = 1.2]).

	Subsection Partial Pressure, mbar								
Sample	5	6	7	8	9	10	11	12	Total Pressure, mbar
#1	0.608	0.407	1.36	2.66	3.14	2.02	0.805	0.209	11.2±0.3
#3	0.639	0.437	1.39	2.60	3.06	2.02	0.807	0.205	11.2±0.1

	Subsection Mole Percent								
Sample	5	6	7	8	9	10	11	12	Ave MW
#1	5.42	3.63	12.1	23.7	28.0	18.0	7.18	1.86	122.3
#3	5.73	3.92	12.4	23.3	27.4	18.1	7.23	1.84	122.0

	Subsection Vapor Density, g/m^3								
Sample	5	6	7	8	9	10	11	12	Total Density, g/m^3
#1	1.63	1.31	5.07	11.3	15.0	10.7	4.68	1.32	51.0
#3	1.72	1.40	5.19	11.0	14.6	10.7	4.70	1.30	50.7

Table A-10. Headspace GC results for the ground test fuel samples at 50°C (0.08 mL [V/L = 274]).

	Subsection Partial Pressure, mbar								
Sample	5	6	7	8	9	10	11	12	Total Pressure, mbar
#1	0.083	0.156	0.851	2.03	2.59	1.74	0.721	0.182	8.35±0.21
#3	0.087	0.172	0.877	2.01	2.57	1.78	0.745	0.198	8.44±0.09

	Subsection Mole Percent								
Sample	5	6	7	8	9	10	11	12	Ave MW
#1	0.994	1.87	10.2	24.3	31.0	20.8	8.63	2.18	126.9
#3	1.03	2.04	10.4	23.8	30.4	21.1	8.83	2.35	127.0

	Subsection Vapor Density, g/m^3								
Sample	5	6	7	8	9	10	11	12	Total Density, g/m^3
#1	0.223	0.500	3.18	8.63	12.4	9.22	4.20	1.15	39.5
#3	0.234	0.552	3.27	8.55	12.3	9.43	4.34	1.26	39.9

Table A-11. Headspace GC results for the ground test fuel samples at 60°C (10 mL [V/L = 1.2]).

	Subsection Partial Pressure, mbar								
Sample	5	6	7	8	9	10	11	12	Total Pressure, mbar
#1	0.731	0.542	1.90	3.89	4.80	3.07	1.38	0.344	16.6±0.1
#3	0.772	0.583	1.96	3.86	4.76	3.28	1.34	0.360	16.9±0.2

	Subsection Mole Percent								
Sample	5	6	7	8	9	10	11	12	Ave MW
#1	4.39	3.25	11.4	23.4	28.8	18.4	8.28	2.06	123.7
#3	4.56	3.45	11.6	22.8	28.1	19.4	7.92	2.13	123.6

	Subsection Vapor Density, g/m^3								
Sample	5	6	7	8	9	10	11	12	Total Density, g/m^3
#1	1.90	1.69	6.88	16.0	22.2	15.8	7.79	2.12	74.4
#3	2.01	1.81	7.09	15.9	22.0	16.8	7.56	2.21	75.5

Table A-12. Headspace GC results for the ground test fuel samples at 60°C (0.08 mL [V/L = 274]).

	Subsection Partial Pressure, mbar								
Sample	5	6	7	8	9	10	11	12	Total Pressure, mbar
#1	0.093	0.174	1.08	2.86	3.97	2.84	1.19	0.343	12.6±0.2
#3	0.088	0.192	1.16	2.84	3.97	2.96	1.34	0.410	13.0±0.3

	Subsection Mole Percent								
Sample	5	6	7	8	9	10	11	12	Ave MW
#1	0.741	1.39	8.60	22.8	31.6	22.6	9.48	2.73	128.6
#3	0.679	1.48	8.95	21.9	30.6	22.8	10.3	3.16	129.1

	Subsection Vapor Density, g/m^3								
Sample	5	6	7	8	9	10	11	12	Total Density, g/m^3
#1	0.242	0.542	3.91	11.8	18.4	14.6	6.72	2.11	58.3
#3	0.229	0.598	4.20	11.7	18.4	15.2	7.56	2.52	60.4

Appendix B

Vapor data calculated from the liquid GC results for the ARCO fuel samples

Table B-1. Liquid GC results for ARCO samples at 40°C (10 mL [V/L = 1.2]).

	Subsection Partial Pressure, mbar								
Sample	5	6	7	8	9	10	11	12	Total Pressure, mbar
Base Jet	0.517	1.09	2.81	1.62	0.910	0.555	0.297	0.109	7.91
2.5% OH	1.27	4.25	9.11	3.71	1.08	0.485	0.259	0.092	20.3
97.5%	0.205	0.141	0.834	1.01	0.852	0.582	0.313	0.113	4.05
95%	0.051	0.020	0.188	0.404	0.638	0.596	0.326	0.118	2.34
92.5%	0.070	–	0.045	0.167	0.385	0.551	0.337	0.122	1.68
90%	0.059	0.047	0.104	0.097	0.245	0.480	0.348	0.128	1.51
87.5%	0.060	0.001	0.003	0.022	0.133	0.379	0.335	0.129	1.06
85%	0.046	0.002	0.003	0.005	0.056	0.284	0.334	0.134	0.865

	Subsection Mole Percent in Vapor								
Sample	5	6	7	8	9	10	11	12	Ave MW
Base Jet	6.54	13.8	35.6	20.5	11.5	7.01	3.76	1.38	108.6
2.5% OH	6.25	21.0	45.0	18.3	5.34	2.40	1.28	0.454	101.6
97.5%	5.07	3.49	20.6	24.9	21.0	14.4	7.73	2.79	120.0
95%	2.17	0.863	8.03	17.3	27.2	25.5	13.9	5.03	131.6
92.5%	4.20	–	2.66	9.99	23.0	32.8	20.1	7.26	137.0
90%	3.90	3.10	6.93	6.41	16.2	31.9	23.1	8.51	136.4
87.5%	5.65	0.106	0.311	2.03	12.5	35.7	31.5	12.1	143.6
85%	5.33	2.59	0.396	0.608	6.42	32.9	38.1	15.5	146.9

Table B-1, cont.

	Subsection Vapor Density, g/m^3								
Sample	5	6	7	8	9	10	11	12	Total Density, g/m^3
Base Jet	1.43	3.60	10.8	7.11	4.48	3.03	1.78	0.714	33.0
2.5% OH	3.51	14.1	35.1	16.3	5.33	2.65	1.56	0.602	79.1
97.5%	0.570	0.468	3.21	4.43	4.20	3.18	1.88	0.739	18.7
95%	0.141	0.067	0.724	1.78	3.14	3.26	1.96	0.771	11.8
92.5%	0.195	--	0.172	0.735	1.90	3.01	2.02	0.797	8.83
90%	0.163	0.155	0.402	0.424	1.21	2.62	2.09	0.840	7.90
87.5%	0.166	0.004	0.013	0.095	0.656	2.08	2.01	0.845	5.86
85%	0.128	0.007	0.013	0.023	0.274	1.56	2.01	0.878	4.88

Table B-2. Liquid GC results for ARCO samples at 40°C (0.08 mL [V/L = 274]).

	Subsection Partial Pressure, mbar								
Sample	5	6	7	8	9	10	11	12	Total Pressure, mbar
Base Jet	0.118	0.536	2.13	1.47	0.880	0.550	0.296	0.109	6.09
2.5% OH	0.309	2.18	7.00	3.37	1.05	0.480	0.258	0.092	14.7
97.5%	0.048	0.070	0.631	0.914	0.823	0.575	0.312	0.113	3.48
95%	0.012	0.010	0.142	0.365	0.616	0.589	0.324	0.118	2.18
92.5%	0.016	--	0.034	0.151	0.372	0.544	0.335	0.122	1.57
90%	0.013	0.023	0.078	0.087	0.236	0.474	0.346	0.128	1.39
87.5%	0.013	--	0.002	0.019	0.128	0.375	0.334	0.129	1.00
85%	0.010	0.001	0.002	0.005	0.054	0.281	0.332	0.134	0.819

	Subsection Mole Percent in Vapor								
Sample	5	6	7	8	9	10	11	12	Ave MW
Base Jet	1.94	8.81	35.0	24.1	14.4	9.04	4.86	1.79	113.6
2.5% OH	2.04	14.6	47.5	23.0	7.14	3.27	1.76	0.626	105.6
97.5%	1.33	1.99	18.1	26.2	23.6	16.5	8.96	3.24	124.1
95%	0.520	0.451	6.49	16.8	28.3	27.1	14.9	5.41	133.9
92.5%	0.987	--	2.12	9.61	23.6	34.6	21.3	7.73	139.8
90%	0.933	1.62	5.64	6.28	17.0	34.2	25.0	9.24	140.3
87.5%	1.30	0.054	0.246	1.94	12.8	37.4	33.3	12.9	147.2
85%	1.21	0.130	0.311	0.577	6.54	34.3	40.6	16.4	150.4

Table B-2, cont.

	Subsection Vapor Density, g/m^3								
Sample	5	6	7	8	9	10	11	12	Total Density, g/m^3
Base Jet	0.333	1.78	8.21	6.43	4.34	3.01	1.78	0.712	26.6
2.5% OH	0.832	7.12	26.9	14.8	5.17	2.62	1.55	0.602	59.6
97.5%	0.128	0.229	2.42	4.01	4.06	3.14	1.87	0.738	16.6
95%	0.031	0.032	0.544	1.60	3.04	3.22	1.95	0.770	11.2
92.5%	0.043	--	0.128	0.663	1.83	2.97	2.01	0.795	8.45
90%	0.036	0.074	0.301	0.382	1.16	2.59	2.08	0.838	7.47
87.5%	0.036	0.002	0.009	0.085	0.632	2.05	2.00	0.844	5.66
85%	0.028	0.004	0.010	0.021	0.264	1.54	2.00	0.877	4.74

Table B-3. Liquid GC results for ARCO samples at 50°C (10 mL [V/L = 1.2]).

	Subsection Partial Pressure, mbar								
Sample	5	6	7	8	9	10	11	12	Total Pressure, mbar
Base Jet	0.711	1.56	4.31	2.62	1.57	1.00	0.566	0.219	12.6
2.5% OH	1.74	6.10	14.0	6.00	1.86	0.876	0.494	0.185	31.2
97.5%	0.283	0.203	1.28	1.63	1.47	1.05	0.596	0.227	6.74
95%	0.070	0.029	0.288	0.654	1.10	1.08	0.621	0.237	4.07
92.5%	0.097	--	0.068	0.271	0.663	0.994	0.641	0.245	2.98
90%	0.081	0.067	0.160	0.156	0.422	0.867	0.662	0.258	2.67
87.5%	0.082	0.002	0.005	0.035	0.229	0.685	0.638	0.259	1.94
85%	0.064	0.003	0.005	0.008	0.096	0.514	0.636	0.270	1.60

	Subsection Mole Percent in Vapor								
Sample	5	6	7	8	9	10	11	12	Ave MW
Base Jet	5.67	12.4	34.3	20.9	12.5	7.98	4.51	1.75	110.4
2.5% OH	5.58	19.5	44.7	19.2	5.97	2.81	1.58	0.593	102.8
97.5%	4.19	3.01	19.0	24.2	21.8	15.6	8.85	3.37	122.0
95%	1.71	0.711	7.07	16.0	27.0	26.4	15.2	5.81	133.2
92.5%	3.25	--	2.29	9.10	22.2	33.4	21.5	8.21	138.7
90%	3.03	2.51	5.99	5.85	15.8	32.4	24.8	9.64	138.6
87.5%	4.26	0.083	0.262	1.80	11.8	35.4	33.0	13.4	145.4
85%	3.98	0.202	0.329	0.533	6.00	32.2	39.9	16.9	148.6

Table B-3, cont.

	Subsection Vapor Density, g/m^3								
Sample	5	6	7	8	9	10	11	12	Total Density, g/m^3
Base Jet	1.91	5.01	16.1	11.2	7.48	5.31	3.29	1.39	51.6
2.5% OH	4.68	19.6	52.1	25.5	8.90	4.64	2.87	1.17	119.4
97.5%	0.759	0.651	4.77	6.95	7.00	5.57	3.47	1.44	30.6
95%	0.188	0.093	1.07	2.78	5.25	5.71	3.61	1.50	20.2
92.5%	0.260	--	0.255	1.15	3.16	5.27	3.73	1.55	15.4
90%	0.218	0.215	0.597	0.665	2.01	4.60	3.85	1.64	13.8
87.5%	0.222	0.005	0.019	0.148	1.09	3.63	3.72	1.65	10.5
85%	0.171	0.010	0.020	0.036	0.457	2.72	3.70	1.71	8.83

Table B-4. Liquid GC results for ARCO samples at 50°C (0.08 mL [V/L = 274]).

	Subsection Partial Pressure, mbar								
Sample	5	6	7	8	9	10	11	12	Total Pressure, mbar
Base Jet	0.127	0.637	2.91	2.25	1.48	0.985	0.562	0.218	9.17
2.5% OH	0.324	2.56	9.57	5.18	1.77	0.859	0.490	0.184	20.9
97.5%	0.050	0.082	0.857	1.40	1.39	1.03	0.592	0.226	5.62
95%	0.012	0.012	0.192	0.559	1.04	1.05	0.616	0.236	3.72
92.5%	0.017	--	0.045	0.231	0.625	0.973	0.636	0.244	2.77
90%	0.014	0.027	0.106	0.133	0.398	0.849	0.657	0.257	2.44
87.5%	0.014	0.001	0.003	0.030	0.216	0.670	0.633	0.259	1.82
85%	0.011	0.001	0.003	0.007	0.090	0.502	0.631	0.269	1.52

	Subsection Mole Percent in Vapor								
Sample	5	6	7	8	9	10	11	12	Ave MW
Base Jet	1.39	6.94	31.7	24.5	16.2	10.7	6.13	2.38	116.4
2.5% OH	1.55	12.2	45.7	24.7	8.44	4.10	2.34	0.881	107.6
97.5%	0.884	1.46	15.2	24.9	24.6	18.3	10.5	4.03	126.6
95%	0.327	0.312	5.17	15.0	27.9	28.3	16.6	6.35	135.7
92.5%	0.602	--	1.64	8.34	22.6	35.1	23.0	8.80	141.4
90%	0.569	1.09	4.35	5.46	16.3	34.8	26.9	10.5	142.4
87.5%	0.764	0.035	0.183	1.62	11.8	36.7	34.7	14.2	148.4
85%	0.705	0.083	0.228	0.477	5.95	33.2	41.6	17.7	151.5

Table B-4, cont.

	Subsection Vapor Density, g/m^3								
Sample	5	6	7	8	9	10	11	12	Total Density, g/m^3
Base Jet	0.342	2.04	10.8	9.56	7.08	5.22	3.27	1.38	39.8
2.5% OH	0.870	8.23	35.7	22.0	8.44	4.55	2.85	1.17	83.8
97.5%	0.133	0.263	3.20	5.95	6.62	5.45	3.44	1.44	26.5
95%	0.033	0.037	0.718	2.38	4.96	5.59	3.58	1.50	18.8
92.5%	0.045	--	0.169	0.983	2.99	5.16	3.70	1.55	14.6
90%	0.037	0.085	0.396	0.566	1.90	4.50	3.82	1.63	12.9
87.5%	0.037	0.002	0.012	0.126	1.03	3.55	3.68	1.64	10.1
85%	0.029	0.004	0.013	0.031	0.431	2.66	3.67	1.70	8.55

Table B-5. Liquid GC results for ARCO samples at 60°C (10 mL [V/L = 1.2]).

	Subsection Partial Pressure, mbar									
Sample	5	6	7	8	9	10	11	12	13	Total Pressure, mbar
Base Jet	0.959	2.20	6.38	4.09	2.59	1.72	1.04	0.420	--	19.4
2.5% OH	2.35	8.61	20.7	9.36	3.08	1.50	0.905	0.354	--	46.8
97.5%	0.381	0.286	1.89	2.55	2.42	1.80	1.09	0.435	0.135	11.0
95%	0.094	0.041	0.427	1.02	1.82	1.85	1.14	0.454	0.141	6.98
92.5%	0.130	--	0.101	0.423	1.10	1.71	1.18	0.469	0.146	5.25
90%	0.109	0.095	0.237	0.244	0.697	1.49	1.21	0.494	0.150	4.73
87.5%	0.111	0.002	0.008	0.054	0.379	1.18	1.17	0.497	0.156	3.55
85%	0.086	0.004	0.008	0.013	0.158	0.882	1.17	0.517	0.163	3.00

	Subsection Mole Percent in Vapor									
Sample	5	6	7	8	9	10	11	12	13	Ave MW
Base Jet	4.94	11.4	32.9	21.1	13.3	8.86	5.35	2.16	--	112.2
2.5% OH	5.01	18.4	44.1	20.0	6.58	3.21	1.93	0.757	--	103.8
97.5%	3.46	2.60	17.2	23.2	22.0	16.4	9.94	3.95	1.23	124.6
95%	1.35	0.586	6.11	14.6	26.0	26.5	16.3	6.50	2.02	135.6
92.5%	2.49	--	1.93	8.06	20.9	32.5	22.4	8.93	2.79	141.4
90%	2.31	2.00	5.01	5.16	14.7	31.5	25.7	10.4	3.17	141.8
87.5%	3.13	0.064	0.211	1.53	10.6	33.1	32.9	14.0	4.40	148.4
85%	2.86	0.152	0.260	0.443	5.28	29.4	38.9	17.2	5.42	151.8

Table B-5, cont.

Sample	Subsection Vapor Density, g/m^3									Total Density, g/m^3
	5	6	7	8	9	10	11	12	13	
Base Jet	2.50	6.86	23.1	16.9	12.0	8.84	5.86	2.58	--	78.6
2.5% OH	6.12	26.8	74.8	38.6	14.3	7.73	5.11	2.18	--	175.7
97.5%	0.993	0.892	6.85	10.5	11.2	9.27	6.17	2.68	0.900	49.5
95%	0.245	0.127	1.54	4.21	8.41	9.50	6.43	2.79	0.939	34.2
92.5%	0.340	--	0.366	1.74	5.07	8.77	6.64	2.88	0.975	26.8
90%	0.284	0.295	0.858	1.01	3.23	7.65	6.86	3.04	0.998	24.2
87.5%	0.290	0.007	0.027	0.225	1.75	6.04	6.61	3.06	1.04	19.0
85%	0.223	0.014	0.028	0.055	0.733	4.53	6.59	3.18	1.08	16.4

Table B-6. Liquid GC results for ARCO samples at 60°C (0.08 mL [V/L = 274]).

	Subsection Partial Pressure, mbar									
Sample	5	6	7	8	9	10	11	12	13	Total Pressure, mbar
Base Jet	0.134	0.731	3.75	3.26	2.37	1.67	1.02	0.417	--	13.4
2.5% OH	0.343	2.96	12.4	7.54	2.83	1.46	0.894	0.353	--	28.8
97.5%	0.052	0.094	1.10	2.03	2.22	1.74	1.08	0.433	0.135	8.88
95%	0.013	0.013	0.247	0.810	1.66	1.78	1.12	0.451	0.141	6.24
92.5%	0.018	--	0.058	0.335	0.999	1.65	1.16	0.466	0.146	4.83
90%	0.015	0.030	0.136	0.193	0.635	1.44	1.20	0.491	0.150	4.28
87.5%	0.015	0.001	0.004	0.043	0.345	1.13	1.15	0.494	0.156	3.35
85%	0.011	0.001	0.004	0.010	0.144	0.850	1.15	0.514	0.162	2.85

	Subsection Mole Percent in Vapor									
Sample	5	6	7	8	9	10	11	12	13	Ave MW
Base Jet	1.01	5.47	28.1	24.4	17.7	12.5	7.67	3.12	--	119.3
2.5% OH	1.19	10.3	43.1	26.2	9.84	5.06	3.11	1.22	--	109.6
97.5%	0.591	1.06	12.4	22.8	24.9	19.6	12.1	4.87	1.52	129.8
95%	0.206	0.213	3.96	13.0	26.6	28.6	18.0	7.22	2.25	138.5
92.5%	0.364	--	1.21	6.93	20.7	34.1	24.0	9.66	3.03	144.0
90%	0.342	0.710	3.19	4.50	14.8	33.5	28.0	11.5	3.49	145.6
87.5%	0.440	0.022	0.128	1.28	10.3	33.9	34.4	14.8	4.66	151.0
85%	0.395	0.050	0.156	0.367	5.05	29.8	40.4	18.0	5.70	154.2

Table B-6, cont.

	Subsection Vapor Density, g/m^3									
Sample	5	6	7	8	9	10	11	12	13	Total Density, g/m^3
Base Jet	0.350	2.27	13.6	13.5	11.0	8.57	5.79	2.57	--	57.6
2.5% OH	0.894	9.20	44.9	31.1	13.1	7.48	5.05	2.17	--	113.9
97.5%	0.137	0.292	3.99	8.37	10.3	8.95	6.09	2.66	0.899	41.7
95%	0.033	0.041	0.896	3.34	7.68	9.17	6.34	2.78	0.937	31.2
92.5%	0.046	--	0.211	1.38	4.63	8.46	6.55	2.87	0.973	25.1
90%	0.038	0.095	0.494	0.796	2.94	7.38	6.76	3.02	0.996	22.5
87.5%	0.038	0.002	0.016	0.177	1.60	5.83	6.52	3.04	1.04	18.2
85%	0.029	0.004	0.016	0.043	0.667	4.37	6.49	3.16	1.08	15.9

Table B-7. Fuel/air mass ratios and fuel mole fractions at nominal loading (V/L = 274 [~3 kg/m^3]) derived from the liquid characterization of the eight ARCO jet fuel samples .

	Fuel/Air Mass Ratio (V/L = 274)					
	40°C		50°C		60°C	
Sample	0 ft[a]	14 kft[b]	0 ft[a]	14 kft[b]	0 ft[a]	14 kft[b]
2.5% OH	0.053	0.092	0.077	0.133	0.107	0.185
Base Jet[c]	0.024	0.042	0.036	0.062	0.054	0.093
97.5%	0.015	0.026	0.024	0.042	0.039	0.067
95%	0.010	0.017	0.017	0.029	0.029	0.050
92.5%	0.007	0.012	0.013	0.022	0.024	0.042
90%	0.007	0.012	0.012	0.021	0.021	0.036
87.5%	0.005	0.009	0.009	0.016	0.017	0.029
85%	0.004	0.007	0.008	0.014	0.015	0.026
	Fuel Mole Fraction (V/L = 274)					
	40°C		50°C		60°C	
Sample	0 ft[d]	14 kft[e]	0 ft[d]	14 kft[e]	0 ft[d]	14 kft[e]
2.5% OH	0.014	0.024	0.020	0.035	0.028	0.048
Base Jet[c]	0.006	0.010	0.009	0.016	0.013	0.022
97.5%	0.003	0.005	0.006	0.010	0.009	0.016
95%	0.002	0.003	0.004	0.007	0.006	0.010
92.5%	0.002	0.003	0.003	0.005	0.005	0.009
90%	0.001	0.002	0.002	0.003	0.004	0.007
87.5%	0.001	0.002	0.002	0.003	0.003	0.005
85%	0.0008	0.001	0.001	0.002	0.003	0.005

[a] Atmospheric mass density (dry air): 1127.4 g/m^3, 40°C; 1092.4 g/m^3, 50°C; 1059.6 g/m^3, 60°C.

[b] Mass ratios at 14 kft were determined by dividing the ratios at sea level by the factor 0.578.

[c] Quarter-scale test #46.

[d] Air molar density: 39.1 moles/m^3, 40°C; 37.9 moles/m^3, 50°C; 36.7 moles/m^3, 60°C. Molar densities were determined from the average molecular weight of air (~28.84 g/mole) and the mass densities of air at the various temperatures.

[e] Fuel mole fractions at 14 kft were determined by dividing the fractions at sea level by the factor 0.578.